Catena 255 (2025) 108983

Contents lists available at ScienceDirect

Catena

journal homepage: www.elsevier.com/locate/catena

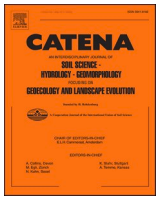

Empirical rainfall thresholds for the triggering of landslides in the NW of the Iberian Peninsula: A state of the art

Pablo Valenzuela [a,*], María José Domínguez-Cuesta [b], Susana Pereira [c], Juan Remondo [d], Txomin Bornaetxea [e], Teresa Vaz [f], Victoria Rivas [g], Jaime Bonachea [d], Alberto González-Díez [d], Eliezer San Millán [d], Carlos Bateira [h], José Luís Zêzere [c]

[a] Grupo de Investigación Geología Ambiental, Cuaternario y Geodiversidad (Q-GEO), Universidad de León 24004 León, Spain
[b] Dpto. de Geología, Universidad de Oviedo 33005 Oviedo, Spain
[c] CEG, Universidade de Lisboa, CEGOT, Dpto. de Geografía, FLUP, Universidade do Porto 4150-564 Porto, Portugal
[d] Dpto. de Ciencias de la Tierra y Física de la Materia Condensada, Universidad de Cantabria, 39005 Santander, Spain
[e] Dpto. de Geografía, Prehistoria y Arqueología, Universidad del País Vasco (UPV/EHU), 01006 Vitoria-Gasteiz, Spain
[f] CEG, IGOT, Universidade de Lisboa, 1600-276, Lisboa, Portugal
[g] Dpto. de Geografía, Urbanismo y Ordenación del Territorio, Universidad de Cantabria, 39005 Santander, Spain
[h] CEG, Universidade de Lisboa, Dpto. de Geografía, FLUP, Universidade do Porto 4150-564 Porto, Portugal

ARTICLE INFO

Keywords:
Landslide
Empirical threshold
Rainfall
Portugal
Spain

ABSTRACT

In this study, we provide a comprehensive review focused on the NW of the Iberian Peninsula identifying a great amount of research works, including 85 empirical rainfall thresholds for the triggering of landslides, some unpublished to date. While the compiled works provide valuable descriptive insights, the thresholds currently have limited predictive capability. The variety of data and approaches used by different authors complicates the comparison of the results and hinders the development of a global understanding of the study area. However, the statistical comparison of four critical accumulated precipitation-duration datasets for the triggering of landslide events from Gipuzkoa, Cantabria, and Asturias in Spain and the N of Portugal highlights a notable similarity in the critical conditions for rainfall-triggered landslides with durations in the range of 3–12 days. Despite the variety of statistical approaches applied, the unexpected similarity aligns with the homogeneous climatic and orographic characteristics across NW Iberia.

1. Introduction

The temporal forecasting of landslides is usually addressed by calculating empirical rainfall thresholds, i.e., equations based on the statistical analysis of critical rainfall conditions defined from a dataset of historical landslide records (Lagomarsino et al., 2015). This common approach represents a simplification, since the statistical treatment of the rainfall records preceding each landslide is prioritized over a more physical-based analysis considering morphological, geological, or hydrological factors (Guzzetti et al., 2007; Zêzere et al., 2015). Thus, the obtained results are often conditioned by constrains such as (1) the reliability of the landslide records source, (2) the size and representativeness of the analysed dataset, (3) the spatial and temporal resolution of the rainfall records, (4) the criterion used to define the critical rainfall, or (5) the type of statistical processing (Valenzuela, 2017; Caracciolo et al., 2017; Segoni et al., 2018; Marra, 2019; Gariano et al., 2020). Therefore, the comparison of thresholds calculated following different approaches may entail some limitations (Lagomarsino et al., 2015; Galanti et al., 2018), even if referring to the same or similar geological and climatic contexts. However, this comparison may be of interest, especially in those areas for which a reduced number of works focused on this subject are available.

The NW of the Iberian Peninsula is an area prone to rainfall-triggered landslides (Wilde et al., 2018), which every year cause significant damages on population and infrastructure (Bonachea et al., 2009; Pereira et al., 2014). The predominant Oceanic climatic conditions and a characteristic rainfall pattern with a winter maximum distinguish this area from (1) the S of the Iberian Peninsula, with a predominant Mediterranean climate, and (2) other peninsular zones with similar average annual rainfall but with summer or autumn maximums and a different

* Corresponding author.
E-mail address: pvalm@unileon.es (P. Valenzuela).

https://doi.org/10.1016/j.catena.2025.108983
Received 21 October 2024; Received in revised form 18 March 2025; Accepted 22 March 2025
Available online 15 April 2025

precipitation distribution over the year, such as the case of the Pyrenees Mountains. Since the late 1980 s, several Portuguese and Spanish research groups have focused on the study of the rainfall as a trigger of landslides. Although some descriptive work has been done (among others: Bateira and Soares, 1997; Domínguez-Cuesta et al., 1999; González-Díez et al., 2022), most of the research has been oriented to the calculation of empirical rainfall thresholds. However, these studies lack spatial and temporal continuity and show methodological disparity, particularly concerning the size and characteristics of the data populations, the criteria to define the triggering rainfall and the statistical processing. These basic differences in the analytical approach generate background noise, rendering difficult to compare the achieved results and to obtain a complete overview of this issue in the area.

The aims of the present work are (1) to perform an in-depth review of the studies focused on the calculation of empirical rainfall thresholds in the NW of the Iberian Peninsula, (2) to describe in detail the different methodologies used in each work, and (3) to discuss the similarities and differences between the critical rainfall conditions defined and the potential for integrating data from different studies to improve the determination of rainfall thresholds at a regional scale.

2. Study area

The NW of the Iberian Peninsula (Fig. 1A) is an area characterized by a rugged orography mainly conditioned by the presence of the Cantabrian Range, with a W–E orientation parallel to the Cantabrian Coast, and the Caurel and Ancares Mountains and the Galaico-Leonés Massif, in the NW corner, which extends to the S through the Galaico-Durienses and Beira-Durienses Mountains (Casas-Sainz and de Vicente, 2009). The narrow coastal strip shows a gentle orography, although the Cantabrian Coast is mainly characterized by the presence of prominent rocky cliffs. The fluvial network of the area shows a general incision pattern, leading to valleys with steep slopes (Tejero et al., 2006). The northern slope of the Cantabrian Range is drained by rivers with relatively small basins, while the Atlantic area is dominated by the large Miño and Duero basins.

From a geological point of view, the NW of the Iberian Peninsula is characterized by a complex geological structure and a great variety of lithologies. The E end of the area (Basque Country and Cantabria) is dominated by the presence of sedimentary rocks from the Mesozoic-Paleogene cover, deformed during the Alpine Orogeny (Alonso et al., 1996). To the W, the cover disappears, allowing the outcrop of Precambrian and Paleozoic rocks from the Iberian Massif, mainly deformed during the Variscan orogeny and subsequently affected by the Alpine deformation (Martínez-González, 2009). From E to W, a geological evolution is apparent from the external zone of the Variscan orogen (Principality of Asturias), with a predominance of sedimentary rocks affected by a thin-skinned tectonic, to the internal zones, with an increase in the metamorphic grade and the intrusion of igneous rocks, frequently affected by intense chemical weathering and predominant in the areas of Galicia and the N of Portugal. Extensive thick Tertiary and Quaternary deposits are not very common in our study area, although these may present local relevance, highlighting those related to fluvial, coastal, glacial, or gravitational processes. Focusing on the current geomorphological dynamics, metric- to decametric-size landslides of different types (rockfalls, slides, flows, or complex mass movements) are frequent along the whole study area. Slope instabilities usually affect the Quaternary deposits or the surficial weathered layer of the bedrock (Bonachea, 2006; Valenzuela, 2017) and are frequently conditioned by anthropic activities or infrastructure. Rainfall has been identified as the

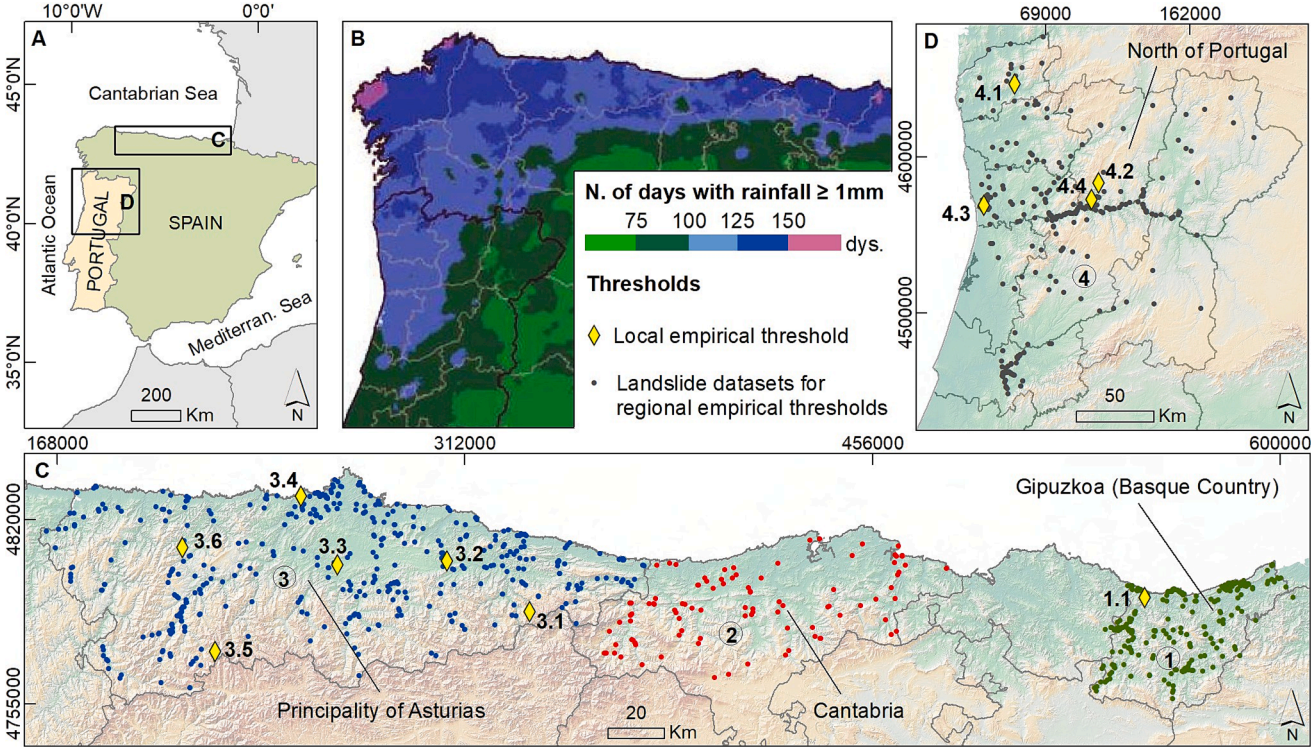

Fig. 1. A Location of the study area. B Average annual number of days with rainfall records ≥ 1 mm in the NW of the Iberian Peninsula. Modified from García Couto et al. (2011). C Landslide event datasets used to calculate regional empirical thresholds for [1] Gipuzkoa (Basque Country), [2] Cantabria, and [3] Principality of Asturias, represented as dots. Zones with local empirical thresholds for the Cantabrian area, represented as rhombus. Basque Country: [1.1] Deba Municipality (Gipuzkoa) – Rivas et al. (2022); Asturias: [3.1] Amieva-Restaño, [3.2] Bargaedo, [3.3] Oviedo, [3.4] Avilés, [3.5] Genestos, and [3.6] Zardaín – Valenzuela et al. (2019). D Landslide event dataset used to calculate regional empirical thresholds for [4] NW Portugal, represented as dots. Zones with local empirical thresholds for the NW Portuguese area, represented as rhombus: [4.1] Casal Soeiro (NW mountains) and [4.2] Vila Real (Douro valley) – Pereira et al. (2012), [4.3] Porto C1 and [4.4] Santa Marta de Penaguião C2 – Vaz (2021).

main triggering factor in this area (Valenzuela et al., 2018a).

According to the Köppen–Geiger classification (Peel et al., 2007; García Couto et al., 2011), two main climatic domains may be differentiated in NW Iberia. The eastern sector is dominated by a temperate climate Cfb, without dry season and with a temperate summer with average temperature ≤ 22 °C, equated to the typical Oceanic conditions. This domain includes the northern hillside of the Cantabrian Range, from the Basque Country to the Principality of Asturias. However, some restricted areas present the variant Cfa, without dry season but with a hot summer characterized by average temperature above 22 °C. Moreover, the highest mountains present the cold climate type D. In contrast, the western sector is dominated by a temperate climate Csb, characterized by a short dry temperate summer (average temperature ≤ 22 °C). This subtype, predominating in central Galicia and northern Portugal, is interpreted as Oceanic conditions in transition towards a Mediterranean climate. Indeed, some areas of the Douro Valley in Portugal present temperate climate Csa, with a dry and hot summer, considered as typical Mediterranean conditions.

The study area is characterized by the abundance of precipitation, with average annual records over 1000 mm year^{-1}, reaching values over 2200 mm year^{-1} in some areas of Galicia, and the N of Portugal. Precipitation is fairly evenly distributed throughout the year, with maximum records during winter (December to February) and minimum records in summer (July and August) (de Luis et al., 2010; García Couto et al., 2011). Average annual number of rainy days is over 100 for records ≥ 1 mm in 24 h and over 75 for records ≥ 10 mm in 24 h, resulting in frequent and meaningful rainy periods. In addition, the frequency of days per year with rainfall ≥ 30 mm in 24 h is over 5, reaching more than 10 days in western Galicia and Portugal, as well as in some areas of the Principality of Asturias, Cantabria, and the Basque Country. Average annual temperature ranges from 5 °C, in the highest mountainous areas, to 10–17.5 °C in the rest of the area (García Couto, 2011; Fig. 1B).

3. Thresholds overview

Here we review the research works on empirical rainfall thresholds developed to date within NW Iberia, focused on the following areas: the Gipuzkoa province (Basque Country), Cantabria, and the Principality of Asturias, within Spain, and the districts of Viana do Castelo, Braga, Oporto, Aveiro, Vila Real, and Viseu, on NW Portugal. We could not find any works focusing on Galicia, even though slope processes are not uncommon in this area. A total of 13 works containing 85 thresholds describing different landslide-triggering rainfall and soil moisture conditions are compiled in the present study. Almost 62 % of them come from works with a wider dissemination: 5 articles, 1 book chapters, and 2 extended abstracts. The remaining 38 % come from 4 PhD thesis and 1 master dissertation. These 85 thresholds are the result of statistical analysis of the triggering conditions, based on data pairs of accumulated precipitation–duration (ED) or precipitation intensity–duration (ID) and expressed as a mathematical equation. An exhaustive account of the works developed in each area is presented below (Fig. 1C and D; Table 4).

Concerning the Basque Country area, Rivas and other authors analyzed the landslides triggered during six multiple occurrence regional landslide events (MORLEs) (October 1953, August 1983, July 1988, October 1992, August 2002, and November 2011) within the Deba municipality (Gipuzkoa), publishing some preliminary result in Rivas et al. (2016) and finally addressing a statistical approach to calculate three ID thresholds (Rivas et al., 2022). Moreover, Bornaetxea and other authors proposed a regional scale approach, performing a statistical analysis of landslide records occurred within the Gipuzkoa province during a 10-year period (January 2006–December 2015) and computing two ED thresholds (Bornaetxea, 2018; Bornaetxea et al., 2018; Fig. 1C).

San Millán (2015) proposed an approach at regional scale for Cantabria. This author addresses the statistical analysis of the rainfall-triggering conditions of a dataset of landslides recorded during a 9-year period (January 2006–February 2015), enabling the calculation of four ID thresholds (Fig. 1C).

Focusing on the Principality of Asturias, Valenzuela et al. (2018b) calculated 16 ID thresholds based on rainfall and soil moisture conditions during two short but intense rainfall episodes: one in June 2010, which resulted in a MORLE affecting the entire region, and another period of intense landslide activity in November–December 2008. Moreover, Valenzuela and other authors have characterized the relation rainfall–landslides during 8 hydrological years, from October 2008 to September 2016, using landslide records from the Principality of Asturias Landslide Database (BAPA for its Spanish acronym; Valenzuela et al., 2017). Valenzuela (2017) determined four regional ED thresholds and eight ED thematic thresholds considering different factors, such as seasonal period, type of slope, type of landslides, or affected substratum. In addition, 18 local ED thresholds have been calculated for different areas of Asturias (Valenzuela et al., 2019; Fig. 1C).

In the case of NW Portugal, Pereira (2009) and Pereira et al. (2010, 2012) initiated a systematic study addressing the computation of thresholds for the areas of Casal Soeiro, in the NW mountains, and Vila Real, in the Douro Valley, based on a landslide inventory compiled for the period 1960–2001. Thus, two ID thresholds and two thresholds combining the rainfall event (72 h) and the antecedent rainfall (10 days) were computed and subsequently updated and transformed into ED thresholds by Zêzere et al. (2015). The most extensive work was developed by Vaz (2021), who benefited from a landslide inventory which covers the period 1865–2010. This work includes 13 local ED thresholds for the Porto area, showing different probabilities of landslide occurrence, 4 local ED thresholds for the Santa Marta de Penaguião area, and 4 regional ED thresholds for mountain and plateaux in the NW of Portugal, although the latter include some landslide events occurred outside the study area of the present work (Fig. 1D).

4. Description of The thresholds

Here we describe and compare the characteristics of the 85 empirical rainfall thresholds abovementioned in detail to understand their significance and representativeness. Three main issues are considered: type of landslide inventories analyzed, meteorological data series used, and methodological approach applied. It should be noted that the landslide inventory of an area can lead to the calculation of several equations.

4.1. Landslide inventories

The statistical thresholds were calculated based on datasets extracted from seven landslide inventories (Table 1). Three of these inventories were specifically collected for the calculation of thresholds, while Pereira (2009), Valenzuela (2017), Vaz (2021) [a in Table 1] and Rivas et al. (2022) used data from databases with wider aims and spatial scales: (1) the database developed by Remondo (2001) and Bonachea (2006) for the Deba municipality, (2) the NPLD database (Pereira et al., 2014), (3) the BAPA database (Valenzuela et al., 2017) and (4) the DISASTER database (Zêzere et al., 2014). Five inventories used press archives as their main data source, one used photointerpretation, and the other one used data from Civil Protection (Table 1). All but one of the inventories (Vaz, 2001; b in Table 1) used auxiliary sources to complete or verify the information from the main source, including data from (1) archival sources (press, technical reports, and scientific publications), (2) population surveys, (3) public security forces and Civil Protection archives, and (4) insurance companies archives. Photointerpretation and mapping data were used in six out of seven inventories to georeference landslides. Fieldwork was used to obtain new data or validate information from other sources in three databases (Table 1).

Four of the reviewed works (Pereira, 2009; Valenzuela, 2017; Bornaetxea, 2018; Vaz, 2021) classified the temporal information in accuracy levels, showing that between 51 and 100 % of the landslides could

Table 1
Characteristics of landslide inventories. Authors; Main/Auxiliary data sources: [Nw] press archives, [T-S] technical reports and scientific publications, [Sf-Cp] security forces and Civil Protection reports, [Ins] insurance companies, [Ph-C] aerial photography and cartography, [S] population surveys, [Fw] field work; Study area; Spatial extension in km^2; Time period in years; Temporal resolution; Landslide type: [Sh] shallow translational slides, [All] including rotational-translational slides, flows and rockfalls; Slope type: [Nat] natural slopes, [Cut] cut slopes, [All] including natural and cut slopes; Number of individual landslide records.

Author		Main source	Aux. sources	Study area	Spatial extension (km^2)	Time period (N. of years)	Temp. resol.	Ld. type	Slop. type	N. of lds.
Bornaetxea, 2018		Nw	Ph-C	Gipuzkoa	Regional (1980)	Jan. 2006–Dec. 2015 (10)	Hourly	All	All	339
Remondo, 2001Bonachea, 2006Rivas et al., 2022		Ph-C	Nw, T-S, Ins, S, Fw	Deba municipality Gipuzkoa	Local (50)	Jan. 1953–Dec. 2015 (60)	Daily	Sh	Nat	1180
San Millán, 2015		Nw	Ph-C	Cantabria	Regional (5326)	Jan. 2006–Feb. 2015 (9)	Daily	All	Cut	150
Valenzuela, 2017		Nw	T-S, Sf-Cp, Ph-C, S, Fw	Asturias	Regional (10 603)	Jan.1980–Dec. 2016 (37)	Daily	All	All	2245
Pereira, 2009		Nw	T-S, Sf-Cp, Ph-C, S, Fw	N Portugal	Regional (29 542)	Jan. 1900–Dec. 2007 (107)	Daily	All	All	624
Vaz, 2021	a	Nw	Ph-C	N Portugal	Regional (29 542)	Jan. 1865–Dec. 2010 (146)	Daily	All	All	894
	b	Sf-Cp	—	N Portugal	Regional (29 542)	Jan. 2006–Mar. 2010 (~4)	Daily	All	All	970

be located at daily scale with reasonable reliability. In addition, 15–22 % of the records present some reference to the moment of the day, and in 13–29 % the time of occurrence is mentioned. In terms of temporal resolution, only one inventory (Bornaetxea, 2018) was developed on an hourly basis. In this case, the time of occurrence had to be estimated based on available information or directly assigned according to some fixed criterion for a relevant percentage of the analyzed landslides (51 %). While in some inventories (Bornaetxea, 2018; Vaz, 2021) only records with exact date of occurrence were considered, other databases (Pereira, 2009; San Millán, 2015; Valenzuela, 2017) also included records with lower levels of temporal accuracy, regardless of their subsequent rejection for the calculation of the thresholds. In such inventories based on photointerpretation (Remondo, 2001; Bonachea, 2006; Rivas et al., 2022), the temporal location of the landslides could not be addressed at daily scale, since the time interval between aerial photographs usually covers months or even years. For this reason, it was necessary to consult complementary archival sources to obtain the precise date of occurrence in those cases in which a relationship extraordinary rainfall event–landslide could be established. In view of the scarcity of reliable time data, the daily scale was considered reasonable for addressing the temporal location of the landslides in six out of seven inventories reviewed.

Regarding landslide location, the inventories based on photointerpretation (Remondo, 2001; Bonachea, 2006) show exact coordinates for all the records represented as points or polygons. The inventories based on press archives also include a relevant percentage of landslides with exact coordinates: 78 % (Pereira, 2009), 60 % (Valenzuela, 2017), 44 % (Bornaetxea, 2018), or 19 % (Vaz, 2021; a in Table 1); records are represented as a dot corresponding to the centroid of the landslide. Some authors (Pereira, 2009; Valenzuela, 2017) benefited from photos and other graphical information present in archival sources and free online cartographic servers (e.g., Google Earth or Google Street View) to refine landslide location. However, most authors considered the location of landslides at municipality scale to be the minimum requirement for their use to compute thresholds, prioritizing temporal over spatial accuracy. For example, Vaz (2021; b in Table 1) only included records located in the parish centroid.

The inventories reviewed in the present work cover time intervals of different lengths. Most of them were compiled during extended periods of time, in the range of 4 to 146 years, registering a great number of individual landslides and multiple landslide events; the exception is the inventory compiled for the Deba municipality (Remondo, 2001; Bonachea, 2006; Rivas et al., 2022), which only considers specific events with similar characteristics. Regarding the spatial dimension, one inventory shows local representativeness, covering the extension of the municipality of Deba, while the remaining inventories were compiled at regional scale, covering large areas defined by some administrative limit (e.g., one or more provinces/districts) but with variable extensions in the range of 1980 to 29 542 km^2. It is worth mentioning that Valenzuela (2017) and Vaz (2021) analyzed the spatial and temporal homogeneity of their inventories, defining those periods were the databases reached a higher level of completeness and representativeness.

Regarding the remaining data usually included in the inventories, three aspects are considered relevant to either select or dismiss the landslide records for the calculation of thresholds: type of landslide, natural or artificial character of the affected slope, and information about the triggering factor. Four out of seven inventories show information about the type of landslide for a variable percentage of the records: 76 % (Pereira, 2009), 66 % (Vaz, 2021; a in Table 1), 47 % (Valenzuela, 2017), and 8 % (Bornaetxea, 2018). In the inventories developed by Remondo (2001) and Bonachea (2006), only shallow translational slides were included from the beginning of the compilation. Valenzuela (2017) included information about the slope for 48 % of the landslides, other inventories only included landslides affecting natural slopes (Remondo, 2001; Bonachea, 2006) or artificial cut slopes (San Millán, 2015), and the remaining databases present no information

related to this matter. Two inventories included information regarding the triggering factor for 68 % (Valenzuela, 2017) and 23 % (Bornaetxea, 2008) of the records. In Pereira (2009) and Vaz (2021) inventories, landslide records with a triggering factor different from rainfall were dismissed from the beginning.

4.2. Meteorological data series

Precipitation data series used to be correlated with the landslide inventories show different structure and characteristics. Most of the works (73 %) considered precipitation records from rainfall gauges, including data in vectorial format with restricted spatial meaning. The number of considered gauges ranged from 1 to 76. The remaining works (27 %) used data series in raster format, representing the precipitation spatial variability over the territory through the interpolation of data from several rain gauges (Table 2). In one case (Rivas et al., 2022), the rasters were developed as part of the work through inverse distance weighted (IDW) interpolation of data from 15 rain gauges. In the cases of Valenzuela et al. (2018b) and Vaz (2021; a in Table 1), the rasters were previously developed by different scientific institutions (Spanish Meteorological Agency, AEMET for its Spanish acronym; Portuguese Institute of Sea and Atmosphere, IMPA for its Portuguese acronym) using kriging interpolation.

Different criteria were used to spatially associate each individual landslide to the most representative data source. In the case of vectorial data, a proximity criterion was considered in five out of eleven works (San Millán, 2015; Valenzuela, 2017; Valenzuela et al., 2018; Bornaetxea, 2018; Vaz, 2021). When different rain gauges were located at similar distances from the landslide, additional selection criteria were considered: altitude, general climatic–geographical conditions, or completeness of the rainfall data series. For the Civil Protection inventory developed by Vaz (2021; b in Table 1), the parish centroid was considered for the application of proximity criteria, since the exact/approximate location of landslides was unknown. In other three cases, some rain gauges were selected as representative of a specific area due to the geographical and climatic characteristics of their location or the completeness of their data series. After that, the selection of the landslides linked to each rain gauge was addressed through the definition of its influence area following different approaches, including the use of an expert criterion (Pereira, 2009), the definition of Thiessen polygons (Valenzuela et al., 2019), or the assessment of the variability of the correlation rainfall–landslide with the distance (Vaz, 2021). For the series in raster format, data were extracted from the cell that coincided with the location of each landslide. The cell size, the radius of the influence area, and the distance landslide–gauge were interpreted as proxies of the spatial resolution of the rainfall data, showing the existence of a certain level of spatial uncertainty from some hundreds of meters to more than 40 km.

The temporal resolution of the rainfall data series is conditioned by the characteristics of the corresponding landslide inventories. Thus, most works used daily precipitation records, except Bornaetxea (2018), who used records per minute converted to hourly scale. The length of the considered rainfall data series does not necessarily coincide with the temporal extension of the landslide inventories; this is conditioned by different factors such as data availability, in the case of the raster data series from the IPMA (Vaz, 2021), or use of methodologies considering the calculation of the return period (Valenzuela et al., 2019). Two works focused on the study of specific landslide events (Valenzuela et al., 2017, Rivas et al., 2022) used short rainfall data series ranging from 2 months to a few days. Two other works (Valenzuela, 2017; Vaz, 2021) considered hydrological or climatological years instead of natural years to delimit the rainfall data series. Finally, Valenzuela et al. (2018b) used daily data of the hydrogeological index Available Water Capacity (AWC) to represent the evolution of soil moisture conditions for periods of 2 and 3 months. These AWC data in raster format (5 km cell size) were extracted from the Daily Water Balance Models developed by the AEMET (Botey and Moreno, 2012).

Table 2
Characteristics of the precipitation data series. Author; .

Author	Source	Time lap	Data structure (N. of gauges)	T accur.	Data selection criteria	Spatial resolution
Bornaetxea, 2018	Euskalmet	Jan. 2006–Dec. 2015 (10 years)	Vectorial data (22)	H	Nearest gauge to the Ld; data gaps < 1 month	—
Rivas et al., 2022	AEMET, Euskalmet, DFG	Jan. 1953–Dec. 2015 (60 years)*	IDW raster (15)	D	Cell coinciding with the Ld	0.1 km Cs
San Millán, 2015	AEMET	Jan. 2006–Feb. 2015 (9 years)	Vectorial data (36)	D	Nearest gauge to the Ld; similar altitude	—
Valenzuela, 2017	AEMET	Oct. 2007–Sep. 2016 (8 hydro. years)	Vectorial data (74)	D	Nearest gauge to the Ld; similar geographical-climatic conditions	0.2–24 km (mean 6.4—km) Ld-ga
Valenzuela et al., 2018b	AEMET	Oct.–Dec. 2008 and May–Jun. 2010 (5 months)	Vectorial data (16–21)	D**	Nearest gauge to the Ld	—
	AEMET	Oct.–Dec. 2008 and May–Jun. 2010 (5 months)	Kriging raster (~800)	D**	Cell coinciding with the Ld	5 km Cs
Valenzuela et al., 2019	AEMET	Oct. 1979–Sep. 2016 (37 hydro. years)	Vectorial data (6)	D	Gauges representative of geographic/climatic conditions; data gaps < 10 %	1.5–48.4 km (mean 18.4 km) Ld-ga
Pereira, 2009	SNIRH, IPMA	Jan. 1960–Dec. 2001 (42 years)	Vectorial data (2)	D	Gauges representative of geographic/climatic conditions; complete data series	≤ 30 km Ld-ga
Vaz, 2021	IPMA	Sep. 1906–Aug. 2006 (100 clim. years)	Vectorial data (1)	D	Gauges representative of geographic/climatic conditions; long-complete data series	≤ 15 km Ld-ga
	IPMA	Sep. 1950–Aug. 2008 (58 clim. years)	Kriging raster (806)	D	Cell coinciding with the Ld	22.2 km Cs (0.2° × 0.2°)
	SNIRH	Jan. 2006–Oct. 2008 (~3 years)	Vectorial data (76)	D	Proximity to the parish centroid	≤ 15 km Ld-ga

Source: [Euskalmet] Basque Meteorological Agency, [AEMET] Spanish Meteorological Agency, [DFG] Provincial Council of Gipuzkoa rain gauge network, [SNIRH] National Water Resources Information System-Portugal, [IPMA] Portuguese Institute of Sea and Atmosphere; Time lap of the precipitation data series: [hydro.] hydrologic year from October to September, [clim.] climatic year from September to August, *only data from some specific date were considered for the calculation of the thresholds; Data structure; Temporal accuracy of the data series: [D] daily accuracy, [H] hourly accuracy, **data with daily accuracy but expressed in h; Data selection criteria; Spatial resolution: [Cs] cell size, [Ld-ga] distance landslide–gauge

4.3. Methodology

Dataset selection

A key issue for the calculation of rainfall thresholds is the selection of the landslide dataset used to perform the statistical analysis. None of the works reviewed considered the complete landslide inventories. Instead, a great variety of criteria was applied in an attempt to ensure the reliability and representativeness of the dataset. Table 3 presents 16 selection criteria considered to define 19 landslide datasets.

The definition of the areas and periods studied allows for a first data selection within the landslide inventories. In the case of the time span, some works focused on specific MORLEs (Valenzuela et al., 2018b; Rivas et al., 2022), while others only used those periods in which the inventory is more complete and representative (Valenzuela, 2017). Vaz (2021) defined the datasets considering an area with common geomorphological characteristics: mountains and plateaux in NW Portugal.

Other group of criteria is based on the available information recorded within the inventories. The spatial and temporal accuracy of the landslide records is considered for the selection of the dataset in those inventories that include records with different accuracy levels (San Millán, 2015; Valenzuela, 2017), dismissing those landslides with unknown date of occurrence. Other authors considered data regarding the landslide triggering, discarding records with a known anthropic cause (Valenzuela, 2017; Bornaetxea, 2018), while landslides with an unknown origin are generally used. Some works defined datasets considering a specific type of landslides, such as Pereira (2009), with only debris flows, or thematic datasets based on the type of landslides and slope or the seasonal period (Valenzuela, 2017). Bornaetxea et al. (2018) dismissed also some landslides due to general doubts about the reliability of the information.

Some aspects linked to the precipitation data series were also used as selection criteria, especially those regarding the existence of certain degree of correlation between rainfall and landslide records. San Millán (2015) and Bornaetxea (2018) discarded landslides without a clear link with rainfall events. San Millán (2015) also dismissed landslides related to rainfall events without rainfall records for the date of occurrence. Similarly, Valenzuela (2017) and Vaz (2021) dismissed those cases in which accumulated precipitation during the 5 days previous to the landslide occurrence was less than 20 mm. The length of the rainfall data series also represented a limiting factor, as in Vaz (2021), resulting in a reduction of the landslide inventory time span used in this study. Moreover, in those works where representative rain gauges were used, the analyzed landslides were limited to those located within the influence area of the gauge, as in Pereira (2009), Valenzuela et al. (2019), and Vaz (2021). In this last study, an additional constraint was applied for those antecedent rainfall conditions defined using raster data series, since the considered landslide datasets were restricted to those raster cells where a number of landslide events equal to or higher than 20 was defined (Vaz, 2021).

Finally, the methodology followed to characterize the critical rainfall

Table 3
Criteria for the selection of the landslide dataset used for the calculation of the statistical thresholds reviewed. Study area; Author: [a] Bornaetxea et al., 2018, [b] Rivas et al., 2022, [c] San Millán, 2015, [d] Valenzuela et al., 2018b, [e] Valenzuela, 2017, [f] Valenzuela et al., 2019, [g] Vaz, 2021, [h] Pereira, 2009; [i] Zêzere et al., 2015; Number of landslides from the original inventory; Selection criteria; Final dataset; Percentage of data used from the original inventory. *Dataset used by Pereira (2009), 14 for Casal Soeiro and 14 for Vila Real, was updated in Zêzere et al. (2015), increasing the number of analyzed landslides in 15 for Casal Soeiro and 19 for Vila Real.

	Study area																		
	Gipuzkoa	Deba municipality	Cantabria	Princip. of Asturias			Zarda in	Genestoso	Avilés	Oviedo	Bargaedo	Amieva	Mount. and plat. in NW Portugal		Casal Soeiro	Vila Real	Porto	Porto C1	Sta. M. Penaguião C2
Author	a	b	c	d	d	e	f	f	f	f	f	f	g	g	h, i	h, i	g	g	g
N. Lds. original inventory	339	1180	150	2245	2245	2245	2245	2245	2245	2245	2245	2245	894	970	624	624	894	894	894
Selection Criteria: Specif. study area													x	x					
Specif. period/event		x		x	x	x	x	x	x	x	x	x							
Exact date						x	x	x	x	x	x	x							
Exact date-coord.			x	x	x	x													
Triggering factor	x			x	x	x	x	x	x	x	x	x							
Landslide type						x									x	x			
Slope type						x													
Data reliability	x																		
P data series length													x					x	x
Correla. Lnd–rainfall	x		x																
P in date of occur.			x																
P > 20 mm in 5 days						x							x	x					
Gauge influence area							x	x	x	x	x	x		x	x	x	x		
P dy.-P ac. < median			x																
P with T > 3 years							x	x	x	x	x	x					x	x	x
Cell ≥ 20 events																		x	x
Final dataset	298	688	33	43	41	463	60	26	72	62	41	43	326	161	15*	19*	82	45	30
% of original inventory	88	58	22	2	2	21	3	1	3	3	2	2	36	17	2	3	9	5	3

Table 4
Empirical thresholds compiled for the NW of the Iberian Peninsula. Author; Study area; Spatial extension: [R] regional, [L] local; Precipitation data structure: [Ve] vectorial, [R] raster; Temporal accuracy: [H] hourly, [D] daily, *daily accuracy with data expressed in h; Number of individual landslides analyzed; Number of landslide events analyzed; Type of threshold: [ED] accumulated precipitation–duration, [ID] precipitation intensity–duration, [E] based on the rainfall event, [A] based on the antecedent rainfall, [EA] based on rainfall event + antecedent rainfall; Equation; Probability of exceedance in percentage; False Alarm rate; Threat Score; Meaning.

Author	Study area	SE	P dat.	T acc.	Lds.	Events	Th. Typ.	Equation	PE%	FA_R	TS	Meaning
Bornaetxea et al., 2018	Gipuzkoa	R	Ve	H	298	298	ED, E	$E = 4.4 \pm 0.7 \cdot D^{0.47 \pm 0.04}$	5			Minimum
		R	Ve	H	298	298	ED, E	$E = 3.0 \pm 0.5 \cdot D^{0.47 \pm 0.04}$	1			Minimum
Rivas et al., 2022	Deba basin	L	Ra	D	688	6	ID, E	$I = 50.73 \cdot D^{-0.428}$	5			Minimum
		L	Ra	D	688	6	ID, E	$I = 66.078 \cdot D^{-0.428}$	25			
		L	Ra	D	688	6	ID, E	$I = 77.165 \cdot D^{-0.428}$	50			
San Millán, 2015	Cantabria	R	Ve	D*	33	33	ID, E	$I = 0.4846 \cdot D^{-0.539}$				Minimum
		R	Ve	D*	33	33	ID, E	$I = 27.109 \cdot D^{-0.621}$				Minimum
		R	Ve	D*	33	33	ID, E	$I = 9.3293 \cdot D^{-1.132}$				Minimum
		R	Ve	D*	97	97	ID, E	$I = 59.19 \cdot D^{-0.488}$				Maximum
Valenzuela et al., 2018	Asturias	R	Ve	D*	43	43	ID, E	$I = 0.70 \cdot D^{-0.25}$	5			Minimum
		R	Ve	D*	43	43	ID, E	$I = 1.20 \cdot D^{-0.25}$	25			
		R	Ve	D*	43	43	ID, E	$I = 2.36 \cdot D^{-0.25}$	50			
		R	Ve	D*	43	43	ID, E	$I = 4.64 \cdot D^{-0.25}$	75			
		R	Ra	D*	43	43	ID, E	$I = 0.94 \cdot D^{-0.27}$	5			Minimum
		R	Ra	D*	43	43	ID, E	$I = 1.49 \cdot D^{-0.27}$	25			
		R	Ra	D*	43	43	ID, E	$I = 2.64 \cdot D^{-0.27}$	50			
		R	Ra	D*	43	43	ID, E	$I = 4.69 \cdot D^{-0.27}$	75			
		R	Ve	D*	41	41	ID, E	$I = 44.89 \cdot D^{-0.80}$	5			Minimum
		R	Ve	D*	41	41	ID, E	$I = 61.71 \cdot D^{-0.80}$	25			
		R	Ve	D*	41	41	ID, E	$I = 91.87 \cdot D^{-0.80}$	50			
		R	Ve	D*	41	41	ID, E	$I = 136.77 \cdot D^{-0.80}$	75			
		R	Ra	D*	41	41	ID, E	$I = 52.03 \cdot D^{-0.84}$	5			Minimum
		R	Ra	D*	41	41	ID, E	$I = 68.17 \cdot D^{-0.84}$	25			
		R	Ra	D*	41	41	ID, E	$I = 95.54 \cdot D^{-0.84}$	50			
		R	Ra	D*	41	41	ID, E	$I = 133.92 \cdot D^{-0.84}$	75			
Valenzuela, 2017	Asturias	R	Ve	D	463	367	ED, E	$E = 1.19 \cdot D^{0.55}$	5			Minimum
		R	Ve	D	463	367	ED, E	$E = 2.15 \cdot D^{0.55}$	20			
		R	Ve	D	463	367	ED, E	$E = 6.92 \cdot D^{0.55}$	50			
		R	Ve	D	463	367	ED, E	$E = 22.71 \cdot D^{0.55}$	80			
		R	Ve	D	92	52	ED, E	$E = 2.61 \cdot D^{0.71}$	20			Dry period
		R	Ve	D	371	315	ED, E	$E = 0.77 \cdot D^{0.72}$	20			Wet period
		R	Ve	D	169	99	ED, E	$E = 6.02 \cdot D^{0.40}$	20			Slides/flows
		R	Ve	D	152	121	ED, E	$E = 0.79 \cdot D^{0.70}$	20			Rockfalls
		R	Ve	D	80	72	ED, E	$E = 5.93 \cdot D^{0.38}$	20			Nat. slope
		R	Ve	D	164	149	ED, E	$E = 1.60 \cdot D^{0.60}$	20			Art. slope
		R	Ve	D	153	128	ED, E	$E = 2.85 \cdot D^{0.51}$	20			Surfic. dep.
		R	Ve	D	183	159	ED, E	$E = 1.42 \cdot D^{0.61}$	20			Bedrock
Valenzuela et al., 2019	Zardaín	L	Ve	D	60	43	ED, A	$E = 6.21 \cdot D + 90.8$	7	0.93	0.07	Minimum
		L	Ve	D	60	43	ED, A	$E = 6.98 \cdot D + 181.3$	28	0.72	0.22	Best-fit
		L	Ve	D	60	43	ED, A	$E = 7.28 \cdot D + 248.7$	100	0	0.07	Maximum
	Genestoso	L	Ve	D	26	21	ED, A	$E = 7.13 \cdot D + 69.5$	2	0.98	0.02	Minimum
		L	Ve	D	26	21	ED, A	$E = 7.71 \cdot D + 132.6$	9	0.91	0.08	Best-fit
		L	Ve	D	26	21	ED, A	$E = 3.05 \cdot D + 298.3$	100	0	0.05	Maximum
	Avilés	L	Ve	D	72	34	ED, A	$E = 4.91 \cdot D + 91$	9	0.91	0.09	Minimum
		L	Ve	D	72	34	ED, A	$E = 4.73 \cdot D + 171.4$	50	0.50	0.32	Best-fit
		L	Ve	D	72	34	ED, A	$E = 5.58 \cdot D + 187.3$	100	0	0.20	Maximum
	Oviedo	L	Ve	D	62	43	ED, A	$E = 4.91 \cdot D + 48.9$	7	0.93	0.07	Minimum
		L	Ve	D	62	43	ED, A	$E = 4.97 \cdot D + 128.2$	52	0.48	0.36	Best-fit
		L	Ve	D	62	43	ED, A	$E = 5.87 \cdot D + 143.9$	100	0	0.19	Maximum
	Bargaedo	L	Ve	D	41	23	ED, A	$E = 6.22 \cdot D + 104.3$	4	0.96	0.04	Minimum
		L	Ve	D	41	23	ED, A	$E = 5.98 \cdot D + 206.6$	7	0.93	0.06	Best-fit
		L	Ve	D	41	23	ED, A	$E = 7.06 \cdot D + 284.1$	100	0	0.04	Maximum
	Amieva	L	Ve	D	43	22	ED, A	$E = 8.81 \cdot D + 96.2$	5	0.95	0.05	Minimum
		L	Ve	D	43	22	ED, A	$E = 8.59 \cdot D + 235.5$	50	0.50	0.35	Best-fit
		L	Ve	D	43	22	ED, A	$E = 10.11 \cdot D + 235.4$	100	0	0.18	Maximum
Pereira, 2009	Vila Real	L	Ve	D	14	8	ED, EA	$E = 1435 \cdot D^{-0.67}$				Minimum
		L	Ve	D	14	8	ID, A	$I = 109 \cdot D^{-0.42}$				Best-fit
	Casal Soeiro	L	Ve	D	14	9	ID, A	$I = 109 \cdot D^{-0.42}$				Best-fit
Zêzere et al., 2015	Vila Real	L	Ve	D	19	11	ED, EA	$E = 2167.9 \cdot D^{-0.755}$				Minimum
		L	Ve	D	19	11	ID, A	$I = 73.72 \cdot D^{-0.438}$				Best-fit
		L	Ve	D	19	11	ED, A	$E = 9.69 \cdot D + 133.31$				Best-fit
	Casal Soeiro	L	Ve	D	15	10	ED, EA	$E = 20290 \cdot D^{-1.089}$				Minimum
		L	Ve	D	15	10	ID, A	$I = 73.72 \cdot D^{-0.438}$				Best-fit
		L	Ve	D	15	10	ED, A	$E = 13.45 \cdot D + 292.53$				Best-fit
Vaz, 2021	NW Mount.	R	Ra	D	326	299	ED, E	$E = 0.5 \cdot D^{0.9}$	5			Minimum
		R	Ra	D	326	299	ED, E	$E = 1.1 \cdot D^{0.9}$	50			
		R	Ve	D	161	152	ED, E	$E = 1.08 \cdot D^{0.72}$	5			Minimum
		R	Ve	D	161	152	ED, E	$E = 2.39 \cdot D^{0.72}$	50			
	Porto	L	Ve	D	82	53	ED, A	$E = 7.7 \cdot D + 57.9$		0.90	0.10	Minimum
		L	Ve	D	82	53	ED, A	$E = 73.4 \cdot D^{0.54}$		0.51	0.33	Best-fit

(continued on next page)

Table 4 (*continued*)

Author	Study area	SE	P dat.	T acc.	Lds.	Events	Th. Typ.	Equation	PE%	FA_R	TS	Meaning
		L	Ve	D	82	53	ED, A	$E = 9.7 \cdot D + 116.4$		0.65	0.24	Best-fit
		L	Ve	D	82	53	ED, A	$E = 7.7 \cdot D + 222.8$		0	0.26	Maximum
		L	Ve	D	82	53	ED, A	$E = 7.7 \cdot D + 100.8$	20	0.80	0.19	
		L	Ve	D	82	53	ED, A	$E = 7.7 \cdot D + 128$	30	0.70	0.26	
		L	Ve	D	82	53	ED, A	$E = 7.7 \cdot D + 153.6$	40	0.60	0.27	
		L	Ve	D	82	53	ED, A	$E = 7.7 \cdot D + 173.3$	50	0.50	0.30	
		L	Ve	D	82	53	ED, A	$E = 7.7 \cdot D + 188.3$	60	0.40	0.30	
	Porto C1	L	Ra	D	45	33	ED, A	$E = 8.83 \cdot D + 54.92$		0.88	0.12	Minimum
		L	Ra	D	45	33	ED, A	$E = 64.53 \cdot D^{0.58}$		0.71	0.22	Best-fit
		L	Ra	D	45	33	ED, A	$E = 10.26 \cdot D + 103.03$		0.72	0.22	Best-fit
		L	Ra	D	45	33	ED, A	$E = 11.25 \cdot D + 165.75$		0	0.12	Maximum
	Penagui. C2	L	Ra	D	30	20	ED, A	$E = 9.6 \cdot D + 81.9$		0.89	0.11	Minimum
		L	Ra	D	30	20	ED, A	$E = 78.26 \cdot D^{0.59}$		0.60	0.29	Best-fit
		L	Ra	D	30	20	ED, A	$E = 10.48 \cdot D + 197.53$		0.61	0.23	Best-fit
		L	Ra	D	30	20	ED, A	$E = 8.46 \cdot D + 375.58$		0	0.30	Maximum

conditions was also used to define the analyzed dataset in some cases. Pereira (2009), Valenzuela et al. (2019), and Vaz (2021) limited the analyzed dataset to those landslides whose antecedent rainfall conditions showed the highest return period, always over 3 years. Furthermore, San Millán (2015) defined a dataset with those landslides whose critical rainfall conditions for the date of occurrence and the previous 5 days were below the respective median, considering the whole analyzed landslides.

As presented in Table 3, the implementation of such selection criteria significantly reduces the number of analyzed landslide records compared with the size of the original inventories. In the case of regional datasets, the number of selected landslide records oscillates between 33 and 463, which represents 17 to 88 % of the original inventories. However, for local-scale approaches, the number of cases included in each dataset ranges from 14 to 82 landslides, which represents 1 to 9 % of the original inventories. In contrast, the landslide dataset representing six MORLE events, selected by Rivas et al. (2022), include 58 % of the landslides from the corresponding inventory.

Definition of landslide event.

Two of the works (Valenzuela et al., 2018b; Rivas et al., 2022) focused on the analysis of specific MORLEs, while the remaining works studied more extended landslide data series, including many landslide events of different sizes. Most authors (Valenzuela, 2017; Valenzuela et al., 2019; Pereira, 2009; Vaz, 2021) defined a landslide event as one or more landslides reported on the same day and related to the same rain gauge or grid cell. In these cases, the number of landslides per event is strongly dependent on the gauge influence areas or the raster cell size. For regional approaches, the use of raster data or a larger number of rain gauges to cover the whole studied territory implied a reduction of the influence areas. Consequently, a great number of events (152 to 367) with a lower average number of landslides per event (1.06 to 1.3) was defined. In contrast, the rate landslide–event is slightly higher in the case of local approaches, in which only one representative rain gauge with a larger area of influence is considered, resulting in a lower number of events (8–76) with a higher average number of landslides per event in the range of 1.2 to 1.8. The remaining works (San Millán, 2015; Valenzuela et al., 2018b; Bornaetxea et al., 2018; Rivas et al., 2022) considered each individual landslide as an event.

Definition of critical rainfall conditions.

The works reviewed here follow three main approaches to determine the critical rainfall conditions by defining: (1) specific rainfall episode that triggered the landslide, (2) longer previous rainfall conditions, and (3) rainfall episode *vs*. antecedent rainfall conditions. In the first case, the rainfall episode is defined as a period of continuous precipitation between the failure and the time when the rainfall event started, while the accumulated precipitation during this period is the critical amount of rainfall. A period with negligible or no rainfall records is usually considered to separate two successive rainfall events, showing different durations depending on seasonal variability. Vaz (2021) used a heuristic criterion, considering rainfall records < 1 mm during 2 days for the dry period (May–September) and 4 days for the wet period (October–April) to separate rainfall episodes in NW Portugal. Similarly, Bornaetxea et al. (2018) considered the absence of rainfall for the same intervals and seasonal periods in Gipuzkoa, defining the episodes automatically using the algorithm proposed by Melillo et al. (2015). Other authors defined the critical period based on the percentage of soil moisture. Valenzuela et al. (2018b) considered the lapse with AWC levels between 99 and 100 % before the initiation of the failure at each landslide location in the Principality of Asturias. The same authors generalized this criterion through the analysis of the number of days without rainfall required to drop those critical AWC levels, defining a period of 1 day for the dry season (June–September) and 3 days for the wet season (October–May; Valenzuela, 2017). In addition, Rivas et al. (2022) considered an expert criterion to define the critical rainfall conditions at the location of each landslide based on available information regarding each specific MORLE event.

Following a different approach, Pereira (2009), Valenzuela et al. (2019), and Vaz (2021) considered the antecedent rainfall for each landslide event. Critical conditions were defined as the rainfall with the highest return period of a series of rainfall values accumulated for different fixed time intervals prior to the landslide occurrence. All authors considered intervals of 1, 2, 3, 4, 5, 10, 15, 30, 40, 60, and 90 days and, additionally, Vaz (2021) considered intervals of 20 and 50 days. In all three works, the return period was calculated using the Gumbel distribution (Gumbel, 1958). Historical rainfall data series equal to or greater than 30 years were used in these analyses.

Finally, the relationship between the accumulated rainfall at the landslide time of occurrence and the accumulated rainfall during the previous days was used, although with some variations, in two other works. Pereira (2009) calculated the accumulated rainfall for 1, 2, and 3 days (triggering conditions) and for 5, 10, 15, 30, 40, 60, 75, and 90 days (preparatory conditions) before the landslide occurrence. Different combinations of triggering–preparatory conditions were iteratively assessed, selecting those with the highest return period. The best correlation with the analyzed landslide events was obtained through the combination 3-day event rainfall and 10-day antecedent rainfall, considered as the critical triggering conditions. San Millán (2015) followed a simpler approach, considering the accumulated rainfall during the day of the landslide occurrence and the previous 5 days; in this case, the antecedent rainfall duration was only conditioned by data availability.

In the approaches followed in Pereira (2009), Valenzuela et al. (2019), and Vaz (2021), not only landslide-triggering conditions, but also those that did not trigger known landslides were defined for the same fixed intervals of days and subsequently used for the threshold calculation. However, some nontriggering conditions were dismissed to clarify the analysis, such as (i) conditions (from 1 to 90 days) from those days with known landslides but not considered as critical due to its low

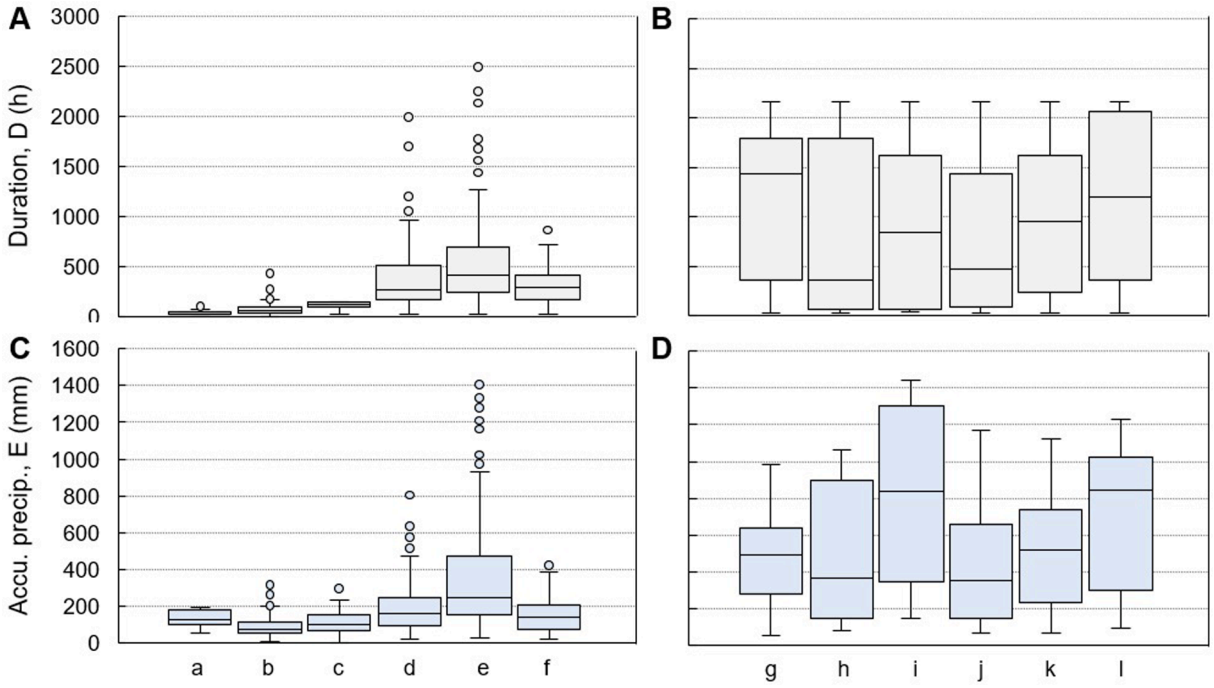

Fig. 2. Comparison between duration (h) and accumulated precipitation (mm) of critical rainfall conditions calculated following different approaches. A, C Considering the rainfall episode: [a] Deba basin (Rivas et al., 2022); [b] Gipuzkoa (Bornaetxea et al., 2018); [c] Cantabria (San Millán, 2015); [d] Principality of Asturias (Valenzuela, 2017); [e and f] Mountains and plateaux NW Portugal (Vaz, 2021). B, D Considering the antecedent rainfall conditions: [g] Principality of Asturias (Valenzuela et al., 2019); [h] Vila Real (Pereira, 2009); [i] Casal Soeiro (Pereira, 2009); [j] Porto (Vaz, 2021); [k] Porto-C1 (Vaz, 2021); [l] Santa Marta de Penaguião-C2 (Vaz, 2021).

return period and (ii) conditions (from 1 to 90 days) of the days following a landslide event with accumulated rainfall values over the minimum thresholds defined for each rain gauge.

The different approaches strongly condition the duration of the critical rainfall periods defined in each case, as shown in Fig. 2. Thus, the critical conditions calculated considering only the triggering rainfall episode present shorter durations. In Gipuzkoa and Cantabria (Fig. 2A: a, b, c), the events show durations in the range of 1–7 days, while in the Principality of Asturias and the NW of Portugal, the events show longer durations in the range of 1–53 days and average duration values of 13–22 days (Fig. 2A: d, e, f). Although less frequent, this first approach also defines events longer than these ranges, as shown by the outliers represented in Fig. 2A. Conversely, approaches considering the antecedent rainfall resulted in longer periods with average durations in the range of 33–49 days (Fig. 2B). The same difference is also observed in the accumulated precipitation during those periods, showing average values from 86 to 349 mm in the first case (Fig. 2C) and from 431 to 794 mm in the second one (Fig. 2D).

Most works used accumulated precipitation–duration (ED) data pairs to describe the critical rainfall conditions, although some authors (Pereira, 2009; San Millán, 2015; Valenzuela et al., 2017; Rivas et al., 2022) used intensity–duration (ID) data pairs, obtaining daily intensity values by dividing the accumulated precipitation by the number of days of the delimited critical period.

4.4. Statistical analysis

Each of the defined landslide datasets was analysed to calculate 85 statistical thresholds expressed as linear or power equations (Table 4) following two main statistical approaches. On the one hand, 35 out of 85 thresholds (41 %) were calculated using a frequentist approach, previously defined by Brunetti et al. (2010) and subsequently modified by Peruccacci et al. (2012) and Gariano et al. (2015), which allows for the characterization of the probability of landslide occurrence. In this case, the calculated functions were assumed as a power law:

$$Y = aX^b$$

where Y is the accumulated event rainfall (E) or the daily rainfall intensity (I), depending on each work, X is the duration (D) of the event rainfall (in hours or days), b is the intercept or scaling parameter, and a defines the slope of the power low curve. The calculation of the parameters a and b was performed using the frequency analysis of the empirical data pair (ED or ID) resulting in known landslides. Data were log-transformed prior to their plotting on a scatter plot. Then, the distribution of the data pairs was fitted throughout the least squared method by means of a linear equation:

$$\log(Y) = \log(a) + b\log(X)$$

Residuals were determined as the difference δ(X) between the logarithm of the empirical Y value, log [Y (D)], of each event and the logarithm of the theoretical Y value corresponding to the best-fit line, log [Y_f (D)], for the same duration.

$$\delta(X) = \log[Y(X)] - \log[Y_f(X)]$$

Then, the probability density function of the residual's distribution was calculated with the Kernel Density Estimation (Venables and Ripley, 2002) by using a Gaussian fit. Based on the function obtained, probability of exceedance lines for different percentages were calculated according to each author: 1 %, 5 %, 20 %, 25 %, 50 % or best-fit, 75 %, and 80 %. The distance between the mean value of the function and the quantile corresponding to each probability (denoted δ* by Brunetti et al., 2010) was used to define the new intercepts for each line. Those new intercepts were calculated by subtracting the corresponding δ* value from the intercept of the best-fit line (a_{50}). However, the b parameter remained unchanged. For this reason, all the calculated probability of exceedance lines are parallels to the best fit line. This approach was used by Valenzuela (2107), Bornaetxea et al. (2018), Vaz

(2019), and Rivas et al. (2022). In the case of Bornaetxea et al. (2018), the methodology was automatically applied through the algorithm developed by Melillo et al. (2015).

On the other hand, in the remaining 50 thresholds (59 %), the authors obtained different equations by applying linear or power regression to all or a part of the ID or ED pairs of critical conditions, represented in a scatter plot, based on the following equations:

$$Y = aX + b$$

$$Y = aX^b$$

where Y is the accumulated event rainfall (E) or the daily rainfall intensity (I), X is the duration (D) of the event rainfall (in hours or days), *b* is the intercept or scaling parameter, and a defines the slope of the function. The adjustment type was selected in each case considering the best correlation coefficient (R^2) values obtained for each line. A simpler approach was applied by San Millán (2015), considering only those ID conditions that caused landslides. In this case, the whole dataset and a subdataset including those data pairs with I and D values under the median were considered, and between 2 and 3 ID data pairs were selected and adjusted through power regression to calculate minimum and maximum regional thresholds. In addition, Pereira (2009), Valenzuela et al. (2019), and Vaz (2021) followed a more complex methodology previously developed by Trigo et al. (2005) and Zêzere et al. (2005, 2008) to establish thresholds at local scale. This approach describes a threshold as a line in the scatter plot that separates rainfall conditions that have triggered landslides from those that have not. Pereira (2009) defined three different datasets considering ID, ED, and 3 days *vs*. 10 days conditions. In all the cases, best-fit thresholds (50 % probability of exceedance) were calculated with lineal and power regression by adjusting only the landslide triggering conditions, although the nontriggering conditions were considered for a visual analysis. In Valenzuela et al. (2019) and Vaz (2021), triggering and nontriggering ED conditions were analyzed together. Thus, best-fit thresholds were calculated considering all ED triggering conditions, while the minimum thresholds were calculated considering only the two lowest ED triggering conditions. Moreover, maximum thresholds were represented considering the two highest ED conditions that did not trigger any known landslide for each dataset. The landslide occurrence probability represented by each threshold was calculated considering all the conditions that triggered and did not trigger landslides over the corresponding line; this probability was expressed as the percentage of the conditions that triggered events over the total conditions above the threshold.

Uncertainty and performance assessment.

Only some of the reviewed works addressed the assessment of the uncertainty linked to the developed thresholds. Valenzuela et al. (2019) and Vaz (2021) interpreted the difference between maximum and minimum thresholds as a way of characterizing the range of uncertainty related to the definition of the functions. Bornaetxea et al. (2018) applied the bootstrapping statistical technique (Peruccacci et al., 2012) to calculate the uncertainty range of the thresholds, showing the level of variability of the resulting functions with respect to the introduced data.

Valenzuela et al. (2019) and Vaz (2021) addressed the quantitative characterization and validation of the performance of those thresholds calculated using both triggering and nontriggering conditions. For this purpose, they used contingency tables and ROC metrics. Four skill scores were calculated by both authors for each threshold following the terminology proposed by Staley et al. (2012): (i) True Positive rate shows the proportion of events correctly predicted; (ii) False Positive rate shows the proportion of positive predictions when the event did not occur, also called false alarms; (iii) False Alarm rate is the ratio between the number of false alarms and the number of true forecasts; and (iv) Threat Score is a measure of the overall performance of the threshold where a perfect model score would equal one (Schaefer, 1990). Additionally, Vaz (2021) calculated the Positive Prediction rate as the inverse of the False Alarm rate. In both works, all but one of the local thresholds corresponding to the best-fit function showed the highest Threat Score values; the exception is the case of Santa Marta de Penaguião-C2, where the highest values is shown by the upper thresholds (Table 4). However, some of these thresholds show elevated False Alarm rate values, especially those with probabilities of exceedance under 50 %. For both authors, the best performance for the forecasting of landslides is observed in those thresholds with probability of exceedance of 50 % and 60 %, when the False Alarm rate and the Threat Score values are more equilibrated (Table 4). Furthermore, Vaz (2021) evaluated the spatial performance of the minimum threshold by analyzing landslides that occurred outside the 15 km-radius influence area around the Porto gauge, confirming its validity up to a distance of 40 km.

Finally, it is worth mentioning that the vast majority of the reviewed statistical thresholds has not been validated with data from subsequent landslide events, nor periodically updated or implemented in early warning system. This lack of validation significantly limits their practical applicability for forecasting purposes. Only the thresholds calculated by Pereira (2009) and Pereira et al. (2010, 2012) have been updated (Zêzere et al., 2015).

5. Comparison of datasets

We selected four approaches for their statistical comparison (San Millán, 2015; Valenzuela, 2017; Bornaetxea et al., 2018; Vaz, 2021; in Table 4). These are the only works in which the thresholds were calculated following reasonably similar methodologies, and together cover most of the proposed study area, being representative of NW Iberia. Thus, the organization of the subsequent analysis in four zones is conditioned by the spatial scope of these works, rather than by geological or climatic criteria. Each of these works includes more than one threshold with different characteristics and meanings (Table 4). All four represent rainfall-triggering conditions defined at regional scale, calculated considering only the rainfall-triggering event and based on the analysis of press archives. Datasets from Gipuzkoa, the Principality of Asturias, and N Portugal consider all the types of landslides, while in Cantabria, only landslides affecting cut slopes are included. However, these works also show relevant differences, such as (1) size of the analyzed database (97, 298, 299 and 367 landslide events), (2) study period (from 8 to 58 years), (3) temporal scale of the rainfall records (hourly data for Gipuzkoa/daily data for all other cases), (4) parameters analyzed (rainfall intensity for Cantabria/rainfall duration for all other cases), and (5) methodology used to define the critical rainfall period (previously detailed in section 4.3), among others. None of these works includes a validation of the thresholds.

The comparison of equations derived from ED and ID data pairs may pose difficulty. Peruccacci et al. (2012) proposed a mathematical relation to converse ID functions in ED functions, only when the original databases present the same temporal scale (daily, hourly); otherwise, the equations cannot be compared in a straightforward manner, rendering necessary their recalculation with data at the same temporal scale. In this case, a new equation, different from that proposed by the original authors, is obtained. Moreover, the statistical method chosen to calculate each fitting function can consider the whole or a part of the critical conditions, determining the probability of occurrence of landslides associated to each equation. When the equations show many differences, as in the present case, their comparison should be discarded, and instead the analysis of the original ED data pairs is recommended. Thus, our analysis focuses on the original ED data pairs derived from each work, which together account for a population of 1061 data.

Most events from Gipuzkoa and Cantabria show durations in the range of 1 to 7 days (24–168 h) and an average accumulated precipitation of 86 and 107 mm, respectively. Duration of the events in the case of the Principality of Asturias and N Portugal shows greater variability,

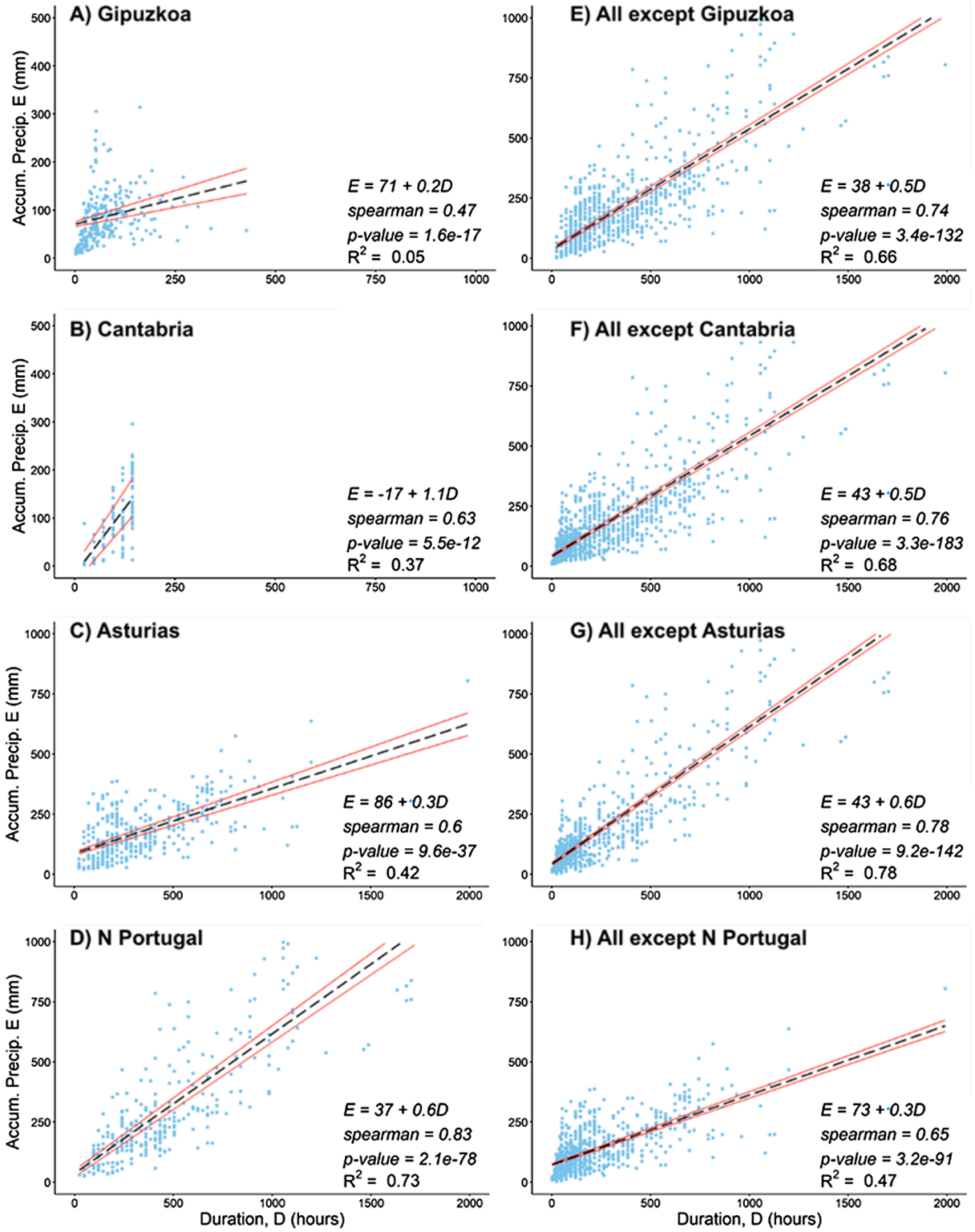

Fig. 3. Linear regression best-fit functions obtained for different ED datasets (dashed black lines); red lines represent the upper and lower standard deviation boundaries of the regression lines. Spearman, p-value and R^2 coefficients are shown for each dataset. Areal datasets: **A** Gipuzkoa; **B** Cantabria; **C** Principality of Asturias; **D** N of Portugal. Remaining datasets: **E** All ED data except Gipuzkoa; **F** All ED data except Cantabria; **G** All ED data except Asturias; **H** All ED data except N of Portugal.

with most values in the range of 1 to 40 days (24–960 h) in Asturias and 1 to 53 days (24–1272 h) in N Portugal, resulting in average accumulated precipitation values of 181 and 349 mm, respectively. In general, events defined for Asturias are shorter than those from Portugal. In contrast, the percentage of events of 1–7 days represents only the 30 % for Asturias and 15 % for N Portugal.

Precipitation duration values (D) in h *vs*. accumulated precipitation during the same period (E) in mm were represented in scatter plots. In

the left insets of Fig. 3 (A, B, C, and D), we represent the datasets from the works focused on each region (areal datasets) and their corresponding regression lines. Likewise, in the right insets (Fig. 3; E, F, G, and H) we exclude one of the datasets, merging the datasets of the remaining areas (remaining dataset) and calculating their regression lines. The upper and lower standard deviations variations (red lines) were calculated for each regression. All eight best-fit regression lines could be interpreted as non-validated thresholds at a 50 % probability of exceedance. However, their main function is to serve as an element of comparison to determine whether each areal dataset falls within the overall variance when considering only the remaining datasets together.

Removal of the outliers from the beginning of the analysis was discarded since the difference between the coefficient of determination values (R^2) of the best-fit lines with and without outliers was not relevant. The frequency distributions of the original datasets show some differences between the datasets and the statistical frequency curves are poorly Gaussian. Consequently, we opted to use Spearman's rank correlation coefficient and checked whether the obtained correlation coefficient was significantly different from 0, computing the associated p-value to assess the significance of the correlations (see Fig. 3). We observed that all p-values were below the threshold of 0.05, indicating that the Spearman coefficient is statistically significant in all cases and

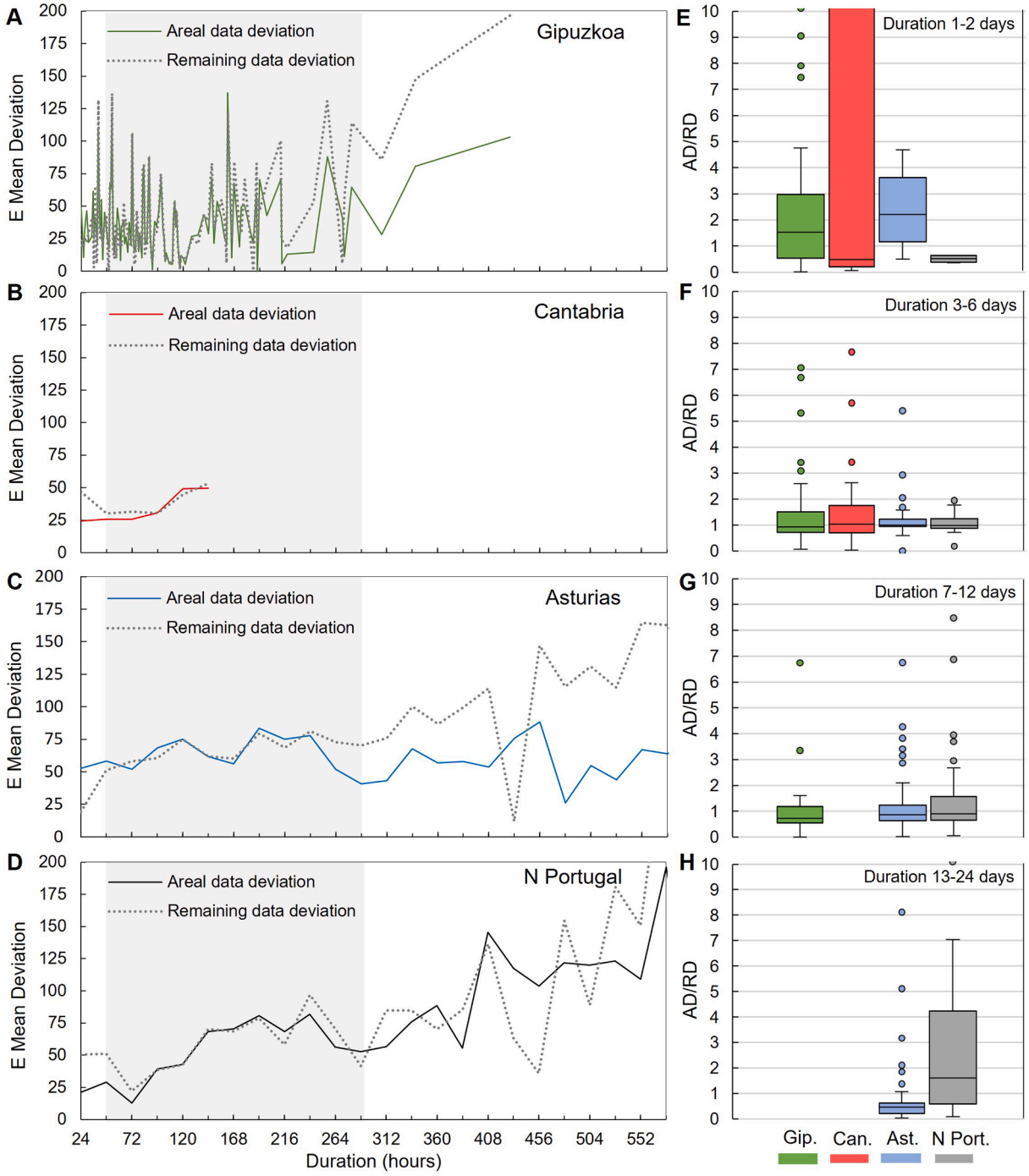

Fig. 4. Mean E areal deviation values *vs.* Mean E remaining deviation values for different durations in (**A**) Gipuzkoa, (**B**) Cantabria, (**C**) Principality of Asturias, and (**D**) N Portugal. Areal dataset deviation/Remaining dataset deviation ratio (AD/RD) for ED events with durations of (**E**) 1–2 days, (**F**) 3–6 days, (**G**) 7–12 days, and (**H**) 13–24 days.

discarding the null hypothesis. Additionally, the calculated coefficient of determination (R2) values obtained provided a general overview of the variance explained by each regression.

The best-fit line obtained for Gipuzkoa shows an R^2 coefficient of 0.05 and a Spearman coefficient of 0.47, consistent with the high dispersion observed in its population data. The trend lines obtained for Cantabria and the Principality of Asturias show R^2 values around 0.4 and associated Spearman coefficients near the value of 0.6. In contrast, the N Portugal dataset shows the best linear fit, reaching an R^2 value of 0.73 with a Spearman coefficient equal to 0.83. The fit of data is better in the case of the joint datasets that include data from N Portugal, reaching R^2 values between 0.66 and 0.78 and Spearman values between 0.74 and 0.78. For the joint dataset without data from N Portugal both, the R^2 value and the Spearman coefficient are lower, with 0.47 and 0.65 respectively. Considering the linear regression functions and the standard deviation values shown in Fig. 3 B and F, Cantabria shows the most relevant differences between the areal dataset and the remaining dataset, which could be due to the small size of the analyzed areal dataset. All best-fit functions show good positive correlations values, slightly less in the case of Gipuzkoa. Despite the general dispersion observed in the eight datasets, which results in the production of fitting functions with highly variable variance, we consider the comparison of these functions useful for evaluating the similarity of each regional data population with the other three selected datasets. Given that landslide-related precipitation datasets naturally exhibit high levels of dispersion, our goal in this comparison was to determine if there is comparable variance between the datasets. Therefore, we conducted an empirical analysis of the residuals. The absolute deviation between the empirical E values and the theoretical E values represented by the best-fit functions was calculated in each case considering the best-fit line of (1) the areal dataset and (2) the remaining dataset. Thus, the ratio of Areal dataset deviation to Remaining dataset deviation (AD/RD) was interpreted as a proxy for the similarity of the variance of the datasets, with maximum similarity approaching a value 1.

Fig. 4 (A, B, C, and D) graphically represents the mean E deviation values for each D value, calculated considering the best-fit line of each areal dataset and of the remaining datasets. In view of the distribution of deviation values for Gipuzkoa data population, both functions show a good fit for events between 39 and 279 h; for events under 39 h, data show a better fit with the trend of the remaining datasets, while for events longer than 279 h, the fit with the Gipuzkoa fitting line is better. Cantabria also shows a good fit between both functions for events in the range of 48 to 144 h, while for events under 48 h, the dataset is better fitted to its own areal trend. The behavior of the Asturian dataset is similar to that observed in Gipuzkoa, with a good coincidence between both functions for periods in the range of 48 to 240 h. Northern Portugal dataset shows a general good fit with their own best-fit line, with a significant coincidence between both functions in the range of 72 to 192 h. In general, the four populations show lower similarity for events of very short and very long durations.

To compare the four data populations, data series were divided into four duration intervals: 1–2 days (24–48 h), 3–6 days (72–144 h), 7–12 days (168–288 h), and 13–24 days (312–576 h); the ratio AD/RD was calculated for each interval to quantify the similarity of data populations and its evolution with the critical rainfall duration (Fig. 4 E, F, G, and H). The rainfall events with durations between 3 and 6 days show 50 % of the AD/RD values closer to 1 and a moderate dispersion, which is particularly reduced in the cases of Asturias and N Portugal, while in Gipuzkoa and Cantabria, AD/RD values show a slightly higher dispersion, always under 2.6. This fact may be interpreted as a relevant similarity of the variance between each areal dataset and the remaining datasets. For events with durations between 7 and 12 days, the range Q1–Q3 of the AD/RD distribution also shows values close to 1, with a reduced dispersion in the cases of Gipuzkoa and the Principality of Asturias, in the range of 0–2, and a wider dispersion in the case of N Portugal, in the range of 0–2.6. Regarding variance, these observations are also interpreted as a relevant level of similarity between areal and remaining datasets. In this second case, no data for Cantabria are available. In contrast, the events with durations between 1 and 2 days and between 13 and 24 days show AD/RD values further away from 1, which may be interpreted as a lower similarity of the ED events of each population.

The results from the analysis performed suggest that the four ED data populations show a remarkable similarity for the critical rainfall events defined for durations between 3 and 12 days (72 and 288 h), which show a similar range of dispersion of the E values. The same analysis shows relevant differences for the events with durations equal or less than 2 days (48 h) and equal or longer than 13 days (312 h). The range of durations between 3 and 12 days includes 485 ED conditions, representing 43 % of total data analyzed.

6. Discussion

The definition of a study area with almost homogeneous climatic and orographic conditions makes it possible to disregard these factors for the analysis, focusing on the influence of the methodological constrains. Thus, our review highlights important differences between the landslide datasets used to calculate the equations: (1) period covered, (2) accuracy of the spatial and temporal location of the landslides, (3) type of landslide, and (4) type slope affected by the landslide (natural or cut-slope). The use of different data sources clearly conditioned the availability and reliability of the information on these topics. Moreover, the different spatial and temporal resolution of the analyzed meteorological data series and the variety of criteria considered to correlate rainfall records and landslide events introduced a relevant level of uncertainty; this fact is particularly striking in the spatial terms, since the distance between the location of the rainfall gauge and the landslide can be longer than 45 km in some cases. In those works where a landslide event is defined as the number of landslides triggered during the same day and spatially related to the same rainfall data source, the size of the event is conditioned by the resolution of the spatial rainfall data. Table 3 presents the high variety of criteria used by the authors to select the landslide records analyzed in their works, further widening the gap between the different landslide datasets and reducing their size.

However, it has been observed that the influence of these physically based constrains could be masked by statistical factors such as: (1) size of the analyzed landslide dataset, (2) methodology used to define the critical rainfall conditions, (3) expression of these critical conditions (ID or ED data pairs), and (4) calculation of the equation. Focusing on the second factor, the consideration of an individual rainfall-triggering episode or more extensive antecedent rainfall conditions strongly affects the results of the analysis. Thus, the works conducted following the first approach resulted in critical conditions of shorter duration and lower accumulated precipitation than those defined following the second approach, as shown in the Fig. 2. The first approach is based on a physical criterion, considering the rainfall event preceding the landslide and directly related to its occurrence. In contrast, the second approach applies a nonphysical criterion, considering an interval of antecedent rainfall with a high return period; this criterion preferentially selects extraordinary events, which ensures a robust relation rainfall–landslide. Considering these basic differences observed, the critical conditions obtained from these two approaches should not be analyzed together.

The performance of the equations was validated through ROC metrics in 35 out of 85 of the compiled thresholds (41 %), all of them local approaches focused on Asturias and N Portugal (Valenzuela et al., 2019 and Vaz, 2001), while in the remaining 50 thresholds, no validation assessments were addressed. Moreover, none of the thresholds has been systematically updated. These two facts significantly limit its usefulness for predictive purposes.

Focusing on the joint analysis of the four selected ED datasets defined by San Millán (2015), Valenzuela (2017), Bornaetxea et al. (2018), and Vaz (2021), the above-mentioned methodological factors also

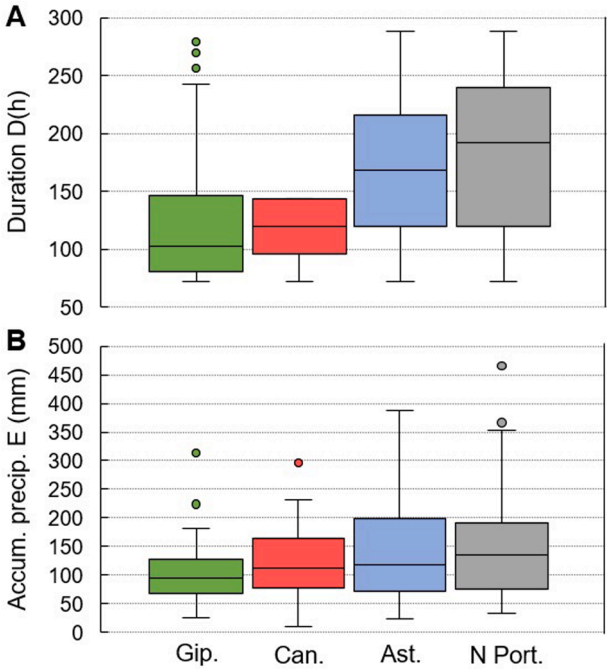

Fig. 5. Duration and accumulated precipitation values for the occurrence of landslides triggered by events of 3 to 12 day duration.

determined the obtained results for each area, distorting the influence of other morphological, geomorphological, geological, or climatic conditions.

Critical rainfall periods defined in Gipuzkoa and Cantabria are of shorter duration (average duration of 3–5 days) compared with those defined for the Principality of Asturias and N Portugal (average duration of 13–22 days), which influences the accumulated precipitation (average rainfall of 76–98 mm for the former and 162–245 mm for the latter). This difference is considered relevant, since in the four cases only the previous rainfall event was considered. In the first two areas, the short duration could be related to the methodology used to define the critical conditions, which considers hourly data in the case of Gipuzkoa and fixed periods of 6 days in the case of Cantabria. In Asturias and N Portugal, the longer duration of the events could be attributed to the use of daily rainfall records, although the ones from N Portugal are even longer than those from Asturias. The reason of this difference could be in the number of days without rainfall considered to define the events in Asturias (1 day for June–September and 3 days for October–May); this criterion is less restrictive than the one used for N Portugal (rainfall records $<$ 1 mm during 2 days for May–September and 4 days for October–April). Moreover, in N Portugal, the landslide database covers a wider period, so that the number of extraordinary rainfall events recorded could be higher than in the other datasets. Four ED datasets show an overall high level of data dispersion, being even higher for events shorter than 3 days and longer than 12 days, as shown in Fig. 4. This could respond to the percentage of events with these durations being significantly different for the four datasets. For example, 48 h-events represent the 36 % in Gipuzkoa and 12 % in Cantabria, but only 4 % and 1 % in Asturias and N Portugal, respectively. Similarly, Gipuzkoa dataset includes only a few events longer than 7 days, and Cantabria includes none, while 69 % and 85 % of the events from Asturias and N Portugal present even longer durations.

These relevant differences between the four datasets are mainly attributed to: (1) the disparity of criteria used to define the critical durations, and (2) the different size and level of completeness of the four landslide databases, in which the very short and long rainfall conditions are often under or overrepresented. Therefore, the previously described characteristics discourage the join analysis of the four ED datasets to calculate new thresholds for NW Iberia. Furthermore they suggest the limited interest of a joint comparison of the equations based on each dataset. We consider that these equations are relevant as descriptors of the critical rainfall conditions in each area. However, the reduced size of the base datasets in some cases along with the general lack of validation analysis and systematic updates hamper its use for further purposes at its current stage of development.

On the other hand, our analysis shows the similarity of the four datasets for the events with durations in the range of 3 to 12 days, with a smaller difference in the number of data (114 in Gipuzkoa, 85 in Cantabria, 186 in Asturias, and 100 in Portugal).

Limiting the comparison to the ED conditions of events in the range of 3–12 days, the same pattern of duration can be observed in the entire data population, with a higher number of short events in Gipuzkoa and Cantabria than those in the Principality of Asturias and N Portugal (Fig. 5A). However, the difference in accumulated precipitation is attenuated with respect to the total dataset, with average values of 95 mm in Gipuzkoa, 111 mm in Cantabria, 118 mm in Asturias, and 135 mm in the N of Portugal (Fig. 5B). Indeed, the similarity is remarkable between the accumulated precipitation values corresponding to the first quartile in four data distributions (67 mm in Gipuzkoa, 78 mm in Cantabria, 73 mm in Asturias, and 76 mm in Portugal). This similarity was unexpected, considering the variety of statistical methodological approaches applied in each work. Leaving aside the bias induced by the critical rainfall events with longer and shorter durations, this result suggests common landslide-triggering conditions for the study area, being consistent with the almost homogeneous geographical and climatic characteristics present throughout the NW of the Iberian Peninsula.

The joint analysis of the four selected ED datasets highlights both the potential and limitations of the available data. While the large number of documented cases allows for the identification of general patterns, the lack of systematic validation and periodic updates limits their predictive applicability. Additionally, statistical factors influencing threshold definitions may obscure the actual role of climatic and geological conditions in landslide triggering. These findings underscore the need for standardized data selection and analysis criteria to enhance threshold reliability.

Despite methodological differences among the studies analyzed, integrating data from the literature could improve the accuracy of

rainfall thresholds for landslide triggering. However, this approach has limitations, as variations in the spatial and temporal accuracy of landslide records and rainfall data introduce uncertainties. In particular, thresholds derived from different methodologies should not be combined indiscriminately, as this could distort their interpretation.

7. Conclusions

In the present work we provide a review that highlights the substantial number of empirical rainfall thresholds (85) calculated for the NW of the Iberian Peninsula in relation to the triggering of landslides. Nonetheless, until now, obtaining an overall view of the knowledge acquired on this subject has been challenging due to the lack of spatial and temporal continuity in these research works, the poor dissemination of some of them, and the variety of methodologies used.

Our analysis highlights the significant interest of the compiled thresholds as descriptors of the different rainfall-triggering conditions across NW Iberia. However, the observed methodological differences and the general absence of validation and systematic update of the compiled equations limit their comparability and practical application for forecasting purposes. In contrast, the comparison of the critical ED conditions calculated at a regional scale for Gipuzkoa, Cantabria, Asturias, and N Portugal for different authors reveals greater similarity than expected—in view of the use of different inventories and analytical methodologies—for events between 3 and 12 days. This fact is consistent with the largely shared geographical and climatic conditions across the NW Iberian Peninsula. Even so, the lack of methodological consistency makes it difficult to use these ED conditions to determine a general threshold for rain-induced landslides triggering as well as a more comprehensive analysis of how physical-based factors influence rainfall-triggered landslides in the area.

Future research progress towards the achievement of operational thresholds for NW Iberia would require: (1) homogenization of the methodological approaches, (2) systematic increase and update of landslide databases, and (3) systematic validation and update of the threshold equations.

CRediT authorship contribution statement

Pablo Valenzuela: Writing – original draft, Supervision, Methodology, Investigation, Formal analysis, Conceptualization. **María José Domínguez-Cuesta:** Writing – original draft, Investigation, Funding acquisition, Formal analysis, Conceptualization. **Susana Pereira:** Writing – review & editing, Methodology, Conceptualization. **Juan Remondo:** Methodology, Funding acquisition, Formal analysis, Data curation. **Txomin Bornaetxea:** Methodology, Investigation, Formal analysis, Data curation. **Teresa Vaz:** Writing – review & editing, Investigation. **Victoria Rivas:** Writing – original draft. **Jaime Bonachea:** Writing – review & editing, Investigation. **Alberto González-Díez:** Investigation. **Eliezer San Millán:** Investigation. **Carlos Bateira:** Investigation. **José Luís Zêzere:** Supervision.

Declaration of competing interest

The authors declare that they have no known competing financial interests or personal relationships that could have appeared to influence the work reported in this paper.

Acknowledgements

The authors would like to thank A. Quirós and A. Escapa for their assistance in the statistical interpretation of the results, as well as the two reviewers for their observations and advice. Part of this research has been funded by (1) RETROCLIFF project, call 2021 for Knowledge Generation Projects founded by the Spanish Ministry of Science and Innovation, the Spanish Research Agency (AEI), and the European Regional Development Found (ERDF) [Ref. MCIU-22-PID2021-122472NB-100], (2) GEOCANTABRICAE project, co-funded by the Foundation for the Promotion of Applied Scientific Research and Technology (FICYT), by the Government of the Principality of Asturias, by the European Union, and by the European Regional Development Found (ERDF) [Ref. SV-PA-21-AYUD/2021/51766], and (3) PAR project "Caracterización de materiales, formas y procesos recientes para mejorar la gestión de los recursos y riesgos geológicos", University of Cantabria [Ref. 29.P209.64004].

References

Alonso, J.L., Pulgar, J., García-Ramos, J., Barba, P., 1996. W5 Tertiary basins and Alpine tectonics in the Cantabrian Mountains (NW Spain). In: Friend, P.F., Dabrio, C.J. (Eds.), Tertiary Basins of Spain: the Stratigraphic Record of Crustal Kinematics. Cambridge University Press, pp. 214–227.

Bateira, C., Soares, L., 1997. Movimentos em massa no norte de Portugal. Factores Da Sua Ocorrência. *Territorium* 4, 63–77.

Bonachea, J. 2006. Desarrollo, aplicación y validación de procedimientos y modelos para la evaluación de amenazas, vulnerabilidad y riesgo debidos a procesos geomorfológicos. *PhD thesis*. 356 pp.

Bonachea, J., Remondo, J., González-Díez, A., Díaz de Terán, J.R., Cendrero, A. 2009. Landslide risk modelling: an experience in northern Spain. In: (J.P. Malet, A. Remaitre and T. Bogaard) *International Conference on Landslide Processes: from Geomorphologic Mapping to Dynamic Modelling. Proceedings*. CERG Editions, 259-264.

Bornaetxea, T., 2018. Methodological approach for landslide analysis in a regional scale. Data collection, susceptibility models and precipitation thresholds. Application in Guipuzkoa Province (basque Country).

Bornaetxea, T., Ormaetxea, O., Antigüedad, I. and Melillo, M. 2018. Landslide & rainfalls: press inventory, conditioning factors characterization and precipitation thresholds for Gipuzkoa province (Basque country). In: Luorenço, L. and Vieira, A. (coord.): *Metodologia de Análise de Riscos através de Estudos de Casos*. Associaçao Portuguesa de Riscos, Prevença e Segurança, 201-222.

Botey, R., Moreno, J., 2012. *Metodología para estimar la humedad del suelo mediante un balance hídrico exponencial diario (Balance hídrico 2)*. AEMET 22, pp.

Brunetti, M.T., Peruccacci, S., Rossi, M., Luciani, S., Valigi, D., Guzzetti, F., 2010. Rainfall thresholds for the possible occurrence of landslides in Italy. *Natural Hazards and Earth System Science* 10, 447–458. https://doi.org/10.1016/j.geomorph.2017.03.031.

Caracciolo, D., Arnone, E., Conti, F.L., Noto, L.V., 2017. Exploiting historical rainfall and landslide data in a spatial database for the derivation of critical rainfall thresholds. *Environmental Earth Sciences* 76, 1–16. https://doi.org/10.1007/s12665-017-6545-5.

Casas-Sainz, A.M., de Vicente, G., 2009. On the tectonic origin of Iberian topography. *Tectonophysics* 474, 214–235.

de Luis, M., Brunetti, M., Gonzalez-Hidalgo, J.C., Longares, L. A., Martin-Vide, J. 2010. Changes in seasonal precipitation in the Iberian Peninsula during 1946–2005. *Global and Planetary Change*, 74 (1), 27-33. DOI: org/10.1016/j.gloplacha.2010.06.006.

Domínguez-Cuesta, M.J., Jiménez Sánchez, M. and Rodríguez García, A. 1999. Press archives as temporal records in the North of Spain: relationships between rainfall and instability slope events. *Geomorphology*, 30 (1-2), 115-123. ISSN: 0169-555X. DOI:10.1016/S0169-555X(99)00049-5.

Galanti, Y., Barsanti, M., Cevasco, A., D'Amato Avanzi, G., Giannecchini, R., 2018. Comparison of statistical methods and multi-time validation for the determination of the shallow landslide rainfall thresholds. *Landslides* 15, 937–952. https://doi.org/10.1007/s10346-017-0919-3.

García Couto, M.A. (Ed.). 2011. *Iberian climate atlas*. Agencia Estatal de Meteorología (España) and Instituto de Meteorología (Portugal), Madrid, Spain, 79 pp.

Gariano, S.L., Brunetti, M.T., Iovine, G., Melillo, M., Peruccacci, S., Terranova, O., Vennari, C., Guzzetti, F., 2015. Calibration and validation of rainfall thresholds for shallow landslide forecasting in Sicily, southern Italy. *Geomorphology* 228, 653–665. https://doi.org/10.1016/j.geomorph.2014.10.019.

Gariano, S.L., Melillo, M., Peruccacci, S., Brunetti, M.T., 2020. How much does the rainfall temporal resolution affect rainfall thresholds for landslide triggering? *Natural Hazards* 100, 655–670. https://doi.org/10.1007/s11069-019-03830-x.

González-Díez, A., Barreda Argüeso, J.A., Valenzuela, P., Del Jesús Clemente, M.D., Diez Barrio, M.A., 2022. La Influencia De Eventos De Precipitación Extremos En El Desencadenamiento De Argayos y En La Meteorización De Taludes Estabilizados; El Ejemplo De La Cuenca Del Saja-Besaya.

Gumbel, E.J., 1958. *Statistics of extremes*. Columbia University Press, New York, USA, p. 395.

Guzzetti, F., Peruccacci, S., Rossi, M., Stark, C.P., 2007. Rainfall thresholds for the initiation of landslides in central and southern Europe. *Meteorology and Atmospheric Physics* 98, 239–267. https://doi.org/10.1007/s00703-007-0262-7.

Lagomarsino, D., Segoni, S., Rosi, A., Rossi, G., Battistini, A., Catani, F., Casagli, N., 2015. Quantitative comparison between two different methodologies to define rainfall thresholds for landslide forecasting. *Natural Hazards and Earth System Science* 15 (10), 2413–2423. https://doi.org/10.5194/nhess-15-2413-2015.

Marra, F., 2019. Rainfall thresholds for landslide occurrence: systematic underestimation using coarse temporal resolution data. *Natural Hazards* 95 (3), 883–890. https://doi.org/10.1007/s11069-018-3508-4.

Martínez-González, F., 2009. Cenozoic tectonic activity in a Variscan basement: Evidence from geomorphological markers and structural mapping (NW Iberian Massif). Geomorphology 107, 210–225.
Melillo, M., Brunetti, M.T., Peruccacci, S., Gariano, S.L., Guzzetti, F., 2015. An algorithm for the objective reconstruction of rainfall events responsible for landslides. *Landslides* 12 (2), 311–320.
Peel, M.C., Finlayson, B.L., McMahon, T.A. 2007. Updated world map of the Köppen-Geiger climate classification. *Hydrology and Earth System Sciences*, 11, 1633-1644. DOI: org/10.5194/hess-11-1633-2007.
Pereira, S. 2009. Perigosidade a movimentos de vertente na Região Norte. *PhD thesis*, 370 pp.
Pereira, S., Zêzere, J.L. and Bateira, C. 2010. Potencialidades dos limiares empíricos de precipitação para o desencadeamento de fluxos de detritos e de lama na região Norte. VI Seminário Latino-Americano de Geografia Física. *II Seminário Ibero-Americano de Geografia Física, Universidade de Coimbra*, 1-15.
Pereira, S., Zêzere, J.L., Quaresma, I.D., Bateira, C., 2014. Landslide incidence in the North of Portugal: Analysis of a historical landslide database based on press releases and technical reports. *Geomorphology* 214, 514–525. https://doi.org/10.1016/j.geomorph.2014.02.032.
Peruccacci, S., Brunetti, M.T., Luciani, S., Vennari, C., Guzzetti, F., 2012. Lithological and seasonal control on rainfall thresholds for the possible initiation of landslides in central Italy. *Geomorphology* 139–140, 79–90. https://doi.org/10.1016/j.geomorph.2011.10.005.
Remondo, J. 2001. Elaboración y validación de mapas de susceptibilidad de deslizamientos mediante técnicas de análisis espacial. *PhD thesis*. 404 pp.
Rivas, V., Remondo, J., Bonachea, J., 2016. Análisis de las relaciones entre precipitación y actividad de deslizamientos en el pasado reciente (NO Guipúzcoa). *Geo-Temas* 16 (1), 633–636.
Rivas, V., Remondo, J., Bonachea, J., Sánchez-Espeso, J., 2022. Rainfall and weather conditions inducing intense landslide activity in northern Spain (Deba, Gipúzcoa). *Physical Geography* 43, 419–439. https://doi.org/10.1080/02723646.2020.1866790.
San Millán, E., 2015. Influencia De Las Precipitaciones En La Ocurrencia De Los Movimientos De Ladera En Cantabria 50, pp.. Master dissertation.
Schaefer, M.G., 1990. Regional analyses of precipitation annual maxima in Washington State. *Water Resources Research* 26 (1), 119–131. https://doi.org/10.1029/WR026i001p00119.
Segoni, S., Piciullo, L., Gariano, S.L., 2018. A review of the recent literature on rainfall thresholds for landslide occurrence. *Landslides* 15 (8), 1483–1501. https://doi.org/10.1007/s10346-018-0966-4.
Staley, D.M., Kean, J.W., Cannon, S.H., Schmidt, K.M., Laber, J.L., 2012. Objective definition of rainfall intensity–duration thresholds for the initiation of post-fire debris flows in southern California. *Landslides* 10, 547–562. https://doi.org/10.1007/s10346-012-0341-9.
Tejero, R., González-Casado, J.M., Gómez-Ortíz, D., Sánchez-Serrano, F. 2006. Insights into the "tectonic topography" of the present-day landscape of the central Iberian Peninsula (Spain). *Geomorphology*, 73(3), 280-294. DOI: geomorph.2005.11.007.
Trigo, R.M., Zêzere, J.L., Rodrigues, M.L., Trigo, I.F., 2005. The Influence of the North Atlantic Oscillation on Rainfall Triggering of Landslides near Lisbon. *Natural Hazards* 36, 331–354. https://doi.org/10.1007/s11069-005-1709-0.
Valenzuela, P. 2017. Landslide triggering in Asturias (NW Spain): rainfall and soil moisture conditions modelling. *Unpublished PhD thesis*, 179 pp.
Valenzuela, P., Domínguez-Cuesta, M.J., Mora García, M.A., Jiménez-Sánchez, M., 2017. A spatio-temporal landslide inventory for the NW of Spain: BAPA database. *Geomorphology* 293, 11–23. https://doi.org/10.1016/j.geomorph.2017.05.010.
Valenzuela, P., Iglesias, M., Domínguez-Cuesta, M.J., Mora García, M.A., 2018a. Meteorological patterns linked to landslide triggering in Asturias (NW Spain): a preliminary analysis. *Geosciences* 8 (1), 18. https://doi.org/10.3390/geosciences8010018.
Valenzuela, P., Domínguez-Cuesta, M.J., Mora García, M.A., Jiménez-Sánchez, M., 2018b. Rainfall thresholds for the triggering of landslides considering previous soil moisture conditions (Asturias, NW Spain). *Landslides* 15, 273–282. https://doi.org/10.1007/s10346-017-0878-8.
Valenzuela, P., Zêzere, J.L., Domínguez-Cuesta, M.J., Mora García, M.A., 2019. Empirical rainfall thresholds for the triggering of landslides in Asturias (NW Spain). *Landslides* 16, 1285–1300. https://doi.org/10.1007/s10346-019-01170-2.
Vaz, T. 2021. Movimentos de vertente desencadeados pela precipitação em Portugal continental. *Unpublished PhD thesis*, 264 pp.
Venables, W.N., Ripley, B.D., 2002. *Modern Applied Statistics with S*. Springer, New York, USA, p. 498.
Wilde, M., Günter, A., Reichenbach, P., Malet, J.P., Hervás, J. 2018. Pan-European landslide susceptibility mapping: ELSUS Version 2. *Journal of Maps*, 14(2), 97-104. DOI: 0.1080/17445647.2018.1432511.
Zêzere, J.L., Pereira, S., Tavares, A.O., Bateira, C., Trigo, R.M., Quaresma, I., Santos, P.P., Santos, M., Verde, J., 2014. DISASTER: a GIS database on hydro-geomorphologic disasters in Portugal. Nat. Hazards 72 (2), 503–532. https://doi.org/10.1007/s11069-013-1018-y.
Zêzere, J.L., Trigo, R.M., Trigo, I.F., 2005. Shallow and deep landslides induced by rainfall in the Lisbon region (Portugal): assessment of relationships with the North Atlantic Oscillation. *Natural Hazards and Earth System Sciences* 5, 331–344. https://doi.org/10.5194/nhess-5-331-2005.
Zêzere, J.L., Trigo, R., Fragoso, M., Oliveira, S., Garcia, R.A.C., 2008. Rainfall-triggered landslides in the Lisbon region over 2006 and relationships with the North Atlantic Oscillation. *Natural Hazard and Earth System Sciences* 8, 483–499. https://doi.org/10.5194/nhess-8-483-2008.
Zêzere, J.L., Vaz, T., Pereira, S., Oliveira, S.C., Marques, R., García, R.A.C., 2015. Rainfall thresholds for landslide activity in Portugal: a state of the art. *Environmental Earth Sciences* 73 (6), 2917–2936. https://doi.org/10.1007/s12665-014-3672-0.